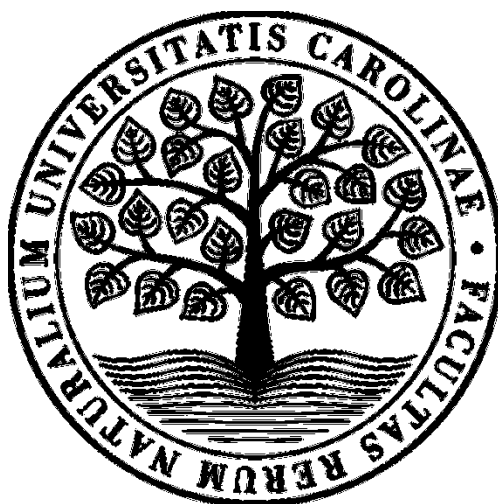


**Univerzita Karlova v Praze
Přírodovědecká fakulta**

Studijní program: Biologie
Studijní obor: Buněčná a vývojová biologie – Fyziologie buňky



Bc. Markéta Sypecká

**Editace leukemických B-buněk pomocí CRISPR/Cas9: hledání cílů miR-155 účastnících
se procesu leukemogeneze**

CRISPR/Cas9 editing of leukemic B-cells: searching for microRNA-155 targets involved in
the process of leukemogenesis

Diplomová práce

Konzultant: Mgr. Elena Golovina

Školitel: RNDr. Karina Savvulidi Vargová, Ph. D.

Praha, 2022

Prohlášení

Prohlašuji, že předkládanou diplomovou práci „Editace leukemických B-buněk pomocí CRISPR/Cas9: hledání cílů miR-155 účastnících se procesu leukemogeneze“ jsem vypracovala samostatně pod vedením RNDr. Kariny Savvulidi Vargové, Ph.D. a s konzultacemi Mgr. Eleny Goloviny, s použitím odborné literatury a dalších informačních zdrojů, které jsou v práci citovány a uvedeny v seznamu použité literatury na konci práce.

V Praze dne 26.4.2022

Markéta Sypecká

Poděkování

Ráda bych poděkovala své školitelce RNDr. Karině Savvulidi Vargové, Ph.D. za trpělivost, věnovaný čas, odborné vedení a tematické připomínky k diplomové práci. Dále také děkuji Mgr. Eleně Golovině za veškerou její pomoc při zpracování mé diplomové práce a v neposlední řadě mým rodičům a přátelům, kteří mě během studia podporovali.

Abstrakt

Editace leukemických B-buněk pomocí CRISPR/Cas9: hledání cílů miR-155 účastnících se procesu leukemogeneze

Úvod: Chronická lymfocytární leukémie (chronická lymfoidní leukémie, CLL) je monoklonální porucha charakterizovaná postupnou akumulací funkčně nekompetentních B-lymfocytů. CLL je nejběžnější formou leukémie u dospělých v západních zemích. Průběh onemocnění se může lišit: někteří pacienti umírají rychle, během 2-3 let od diagnózy, převážně kvůli komplikacím z CLL, ale většina pacientů žije 5-10 let. S progresí nemoci stoupá exprese miR-155, která je označována jako oncomiR.

MikroRNA (miRNA) představují negativní regulátory genové exprese. MiR-155 ovlivňuje geny, které se účastní leukemogeneze a buněčného cyklu. A je známo, že miR-155 (podobně jako i jiné miRNA) potlačuje své cíle.

Předpokládali jsme, že úpravou genů v CLL bunkách odblokujeme cíle miR-155 a zjistíme korelaci mezi těmito cíli (známými a neznámými) s leukemogenezí CLL.

Metody: Metodu, kterou jsme použili pro editaci genů, je CRISPR/Cas9, která umožňuje odstranit sekvenci maturované miR-155 v genomu leukemických B-buněk. K přenosu plasmidu CRISPR/Cas9 byla využita metoda nukleofekce. K identifikaci buněčných klonů s úspěšnou transfekcí plasmidu CRISPR/Cas9 došlo pomocí FACS a míra exprese jednotlivých genů byla měřena pomocí qRT-PCR.

Výsledky: Podařilo se nám izolovat klon, který nese jednu alelickou delecii (miR-155 -/+) v sekvenci pro zralou miRNA-155; určit změny exprese v sadě validovaných cílů miRNA-155 v tomto miR-155 -/+ monoalelickém klonu a porovnat transkripty ve zdravých B-buňkách, buněčných liniích CLL MEC-1 (agresivní CLL stupeň) a HG-3 (střední CLL stupeň). Také se nám podařilo identifikovat potenciální nové cílové geny miR-155, a to *ISG15* a *RPS29*.

Závěr: Naše výsledky mohou být využity pro další studium metabolických drah leukemogeneze a dalších rakovinných onemocnění.

Klíčová slova: microRNA-155, CRISPR/Cas9, B-buňky, leukemogeneze, genová exprese.

Abstract

CRISPR/Cas9 editing of leukemic B-cells: searching for microRNA-155 targets involved in the process of leukemogenesis

Introduction: Chronic lymphocytic leukemia (chronic lymphoid leukemia, CLL) is a monoclonal disorder characterized by a progressive accumulation of functionally incompetent B-lymphocytes. CLL is the most common form of leukemia found in adults in Western countries. Course of the disease can differ: some patients die rapidly, within 2-3 years of diagnosis, mainly due to complications from CLL, but most patients live 5-10 years. However, with disease progression significantly increases level of miR-155, which is known as oncomiR.

MicroRNAs (miRNAs) represent negative regulators of gene expression. MiR-155 affects genes, which are involved in leukemogenesis and cell cycle. And it is known, that miR-155 suppresses its targets (similarly as other miRNAs).

We hypothesized that by gene editing of CLL cells we unblock miR-155 targets and find out correlation between these targets (known and unknown) with CLL leukemogenesis.

Methods: We used CRISPR/Cas9 method for gene editing, which enables the deletion of mature miR-155 sequence in the genome of leukemic B-cells. CRISPR/Cas9 plasmid was transferred to the leukemic B-cell cell line HG-3 via nucleofection. Clones with successful transfer of plasmid were sorted via FACS and further the level of expression of target genes was measured by qRT-PCR.

Results: We achieved to isolate clone that bears monoallelic deletion (miR-155-/-) from the sequence for mature miRNA-155; determine expression changes in set of validated miRNA-155 targets in this miR-155-/- biallelic clone and compare transcriptomes in healthy B-cells, CLL cell lines MEC-1 (aggressive CLL stage) and HG-3 (intermediate CLL stage). We also found two new potential targets of miR-155 – *ISG15* and *RPS29*.

Conclusion: Our findings can be used for further studies of metabolic pathways in leukemogenesis and different cancerous diseases.

Keywords: microRNA-155, CRISPR/Cas9, B-cells, leukemogenesis, gene expression

Contents

Abstrakt	5
Abstract	6
List of Abbreviations.....	1
1. Introduction	3
1.1 Chronic Lymphocytic Leukemia (CLL).....	3
1.1.1 CLL Diagnosis, Prognosis, Treatment	3
1.2 Characteristics of microRNAs.....	5
1.2.1 Discovery	5
1.2.2 Biogenesis of miRNAs.....	5
1.2.3 Mechanism of function.....	7
1.2.4 MiR-155 expression in hematopoetic cells	7
2. Hypothesis.....	15
2.1 Aims of the thesis	15
2.2 Specific aims of the thesis	15
3. Material and Methods.....	16
3.1 Material.....	17
3.1.1 Biological material	17
3.1.2 Chemicals and buffers	18
3.1.3 Instruments	19
3.2 Methods	19
3.2.1 Cultivation of HG-3 cell line.....	19
Transfection of HG-3 Cells by Amaxa nucleofector	20
3.2.2 FACS – Fluorescence Activated Cell Sorting and Gaining of the Clones.....	20
3.2.3 Sequencing	22
Gene expression	24
3.2.4 Statistical analysis	26

4. Results	27
5. Discussion	43
6. Conclusion.....	53
7. References	54

List of Abbreviations

CDKN1A	Cyclin Dependent Kinase Inhibitor 1A
CLL	chronic lymphocytic leukemia
DMSO	dimethylsulfoxid
FACS	fluorescence activated cell sorting
FBS	fetal bovine serum
FCR	combination of drugs: fludarabine, cyclophosphamide, rituximab
GNB4	G Protein Subunit Beta 4
HIST1H2AC	Histone H2A type 1-C
HMGCS1	Hydroxymethylglutaryl-CoA synthase
ISG15	ISG15 Ubiquitin Like Modifier
LDHA	Lactate Dehydrogenase A
LMNA	Lamin A/C
miR-155	microRNA - 155
MX1	MX Dynamin Like GTPase 1
NSNU5	NOP2/Sun RNA Methyltransferase 5
PBS	phosphate buffered saline
PDCD4	Programmed Cell Death 4
PNN	Pinin, Desmosome Associated Protein
PRKAR1A	Protein Kinase CAMP-Dependent Type I Regulatory Subunit Alpha
PSMG2	Proteasome Assembly Chaperone 2
PU.1	Transcription factor PU.1
qPCR	quantitative polymerase chain reaction
RPS29	Ribosomal Protein S29
RRP15	Ribosomal RNA Processing 15 Homolog

SRSF1	Serine And Arginine Rich Splicing Factor 1
THRAP 3	Thyroid Hormone Receptor Associated Protein 3
TMSB4X	Thymosin Beta 4 X-Linked
VIM	Vimentin

1. Introduction

1.1 Chronic Lymphocytic Leukemia (CLL)

Chronic Lymphocytic Leukemia (CLL) is an incurable disease, and one of the most frequent leukemias in developed countries. CLL is most frequently diagnosed among people aged 65–74, the median age at diagnosis is 70. (Chronic Lymphocytic Leukemia - Cancer Stat Facts, b.r.)

1.1.1 CLL Diagnosis, Prognosis, Treatment

Chronic Lymphocytic Leukemia is characterised by the accumulation of mature and CD5-positive B-cells – found in peripheral blood, bone marrow, spleen, and lymph nodes. CLL cells express following antigens CD19, CD20, and CD23 (Rozman & Montserrat, 1995). The most common revelation of Chronic Lymphocytic Leukemia is incidental discovery, mostly by routine examination. CLL is diagnosed by an elevated B-cell count in peripheral blood, estimated at more than 5000 B-cells per μL (Fig. 1). Which is 10-100 times higher than the usual concentration by a healthy person (Concentration of B cells in blood - Human Homo sapiens - BNID 103556, b.r.). The elevated count can be caused by other reasons e.g., infection. These reasons for lymphocytosis and lymphadenopathy have to be excluded, therefore immunophenotyping of peripheral blood is performed. In the case of immunophenotyping not being enough to diagnose, a biopsy of lymph nodes is executed.

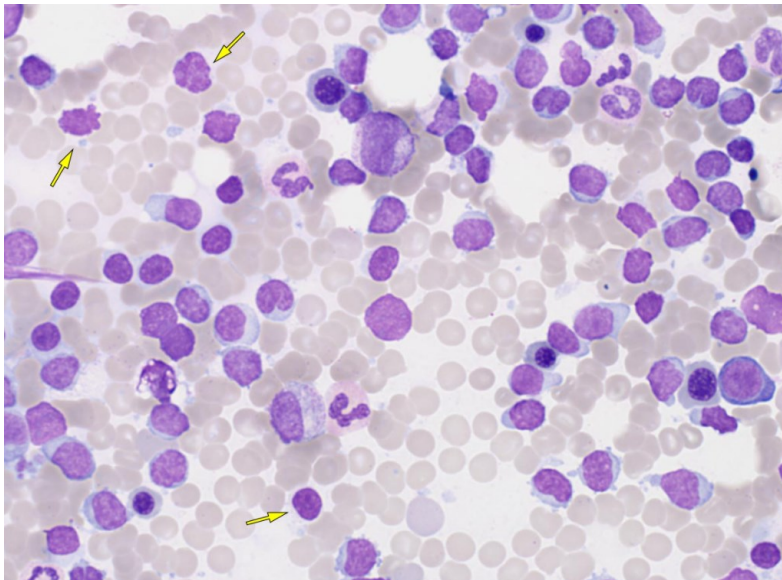


Fig. 1 Blood smear of bone marrow. Smudge cells, typical for chronic lymphocytic leukemia are shown in the picture by yellow arrows. (Picture was adapted from *Atlas of Haematological Cytology*, b.r.)

Prognosis

An international prognostic index for patients with chronic lymphocytic leukemia (CLL-IPI) („An International Prognostic Index for Patients with Chronic Lymphocytic Leukaemia (CLL-IPI)", 2016) was created to separate patients into four risk groups with a different chance of survival and planning of treatment – Low risk, Intermediate risk, High risk, and Very high risk. Separation into these four groups was performed based on specific genomic changes and chromosomal aberrations. Initial and most frequent aberration is the deletion of the 13q chromosome, which is present in 55 % of cases and trisomy of 12 chromosome. In more advanced stages, deletions of chromosome 11q and 17p occur (Rozman & Montserrat, 1995).

Genetic and molecular biology markers can be used for identification of the risk of progression and survival, which is complementary to the staging system. Mutations in specific genes vary according to the stage of the disease, for example, *TP53* aberrations specifically occur by aggressive disease.

Besides the abovementioned genetic markers the CLL progression is also characterised by occurrence of ZAP-70, CD38 molecules and on the mutation status of IgVH. Where the favorable CLL stage is described by ZAP-70-, CD38-, mutated IgVH and the adverse CLL stage is described by expression of ZAP-70, CD38 and unmutated status of IgVH (Chiorazzi *et al.*, 2005)

Treatment

In the early stage of the disease, asymptomatic patients are monitored without therapy until disease progression. Basically, clinicians follow the rule "watch and wait"

Treatment of patients starts based on the Rai and Binet staging system and present symptoms, e.g., marrow failure, thrombocytopenia, unintentional weight loss.

Different types of chemoimmunotherapy drugs are used based on the patient's fitness level and presence of *TP53* aberration. Treatment by a combination of drugs, such as anti-CD20 monoclonal antibody rituximab, fludarabine, and cyclophosphamide (FCR) helps the treatment and prolongs survival of patients. Patients with FCR treatment achieved the longest median progression-free survival, which leads to chemoimmunotherapy with FCR is the first-line standard care for physically fit patients (Cramer *et al.*, 2016).

Patients with *TP53* aberration have a very aggressive disease course and respond poorly to chemoimmunotherapy. The outcome improved with the introduction of ibrutinib, idelalisib, and venetoclax, all of them act independently of the p53 pathway.

Choosing the right pathway for treatment may be difficult because of so many options. Therefore parameters that are considered include fitness, age, comorbidities, and genetic status of *TP53* (Eichhorst et al., 2015).

Duration of remission varies however, 86,1 % of patients survive 5 years after the diagnosis of CLL (*Chronic Lymphocytic Leukemia - Cancer Stat Facts*, b.r.). Patients are regularly monitored and when symptoms occur, second-line treatment starts. The sooner relapse appears the poorer prognosis the patient has.

1.2 Characteristics of microRNAs

MicroRNAs (miRNAs) represent single stranded non-coding RNAs (ncRNAs) found in all kingdoms (plants, animals and viruses) and 18-25 nucleotides long (Mashima, 2015). MiRNAs are evolutionarily conserved among species that underlie their importance in biological processes (Bartel DP et al, 2018). The function of miRNAs lies in the regulation of gene expression by suppressing newly synthesised proteins through inhibition or destabilisation of mRNA (messengerRNA) in eukaryotes (Mashima, 2015).

1.2.1 Discovery

The first miRNA was discovered in 1993 by Ambros's and Ruvkun's groups in *Caenorhabditis elegans*, specifically lin-4, which is crucial in the larval development of *C. elegans* (Almeida et al., 2011). In 2000 was discovered second miRNA and there began outbreak of discoveries connected to miRNAs. Such as importance of DICER protein in miRNA pathway (Grishok et al., 2001; Hutvagner et al., 2001), connection between overexpression of miRNAs and cancer. Using anti-miR for therapy. Overexpression of a single miR is sufficient to cause cancer (O'Donnell et al., 2005).

Silencing of the target gene is based on Watson-Crick base pairing of the miRNA with 3'UTR of the gene.

1.2.2 Biogenesis of miRNAs

Most mammalian miRNAs are transcribed in the genome at first in the form of long primary transcripts (pri-miRNAs) by RNA polymerase II. The pri-miRNAs consist of cap

structure at the 5' end, one or more hairpin structures and polyadenylated 3' end. Pri-miRNAs can be spliced in more ways, which leads to generating more than one functional miRNA (Carthew and Sontheimer, 2009). In the nucleus, the pri-miRNAs are processed by RNase II endonuclease III Drosha enzyme and DGCR8/Pasha protein, a double-stranded RNA-binding domain protein. After the excision precursor-miRNA (pre-miRNA) is formed and exported from the nucleus by Exportin 5 protein. After the displacement of pre-miRNA into the cytoplasm, pre-miRNA is cleaved by Dicer protein (Carthew & Sontheimer, 2009). The pre-miRNA in duplex form binds to a protein of the Argonaute (Ago) family to build an RNA Induced Silencing Complex (RISC). Regulation of miRNA biogenesis has not been extensively studied yet. The process of miRNA biogenesis described above shows **Fig. 2**.

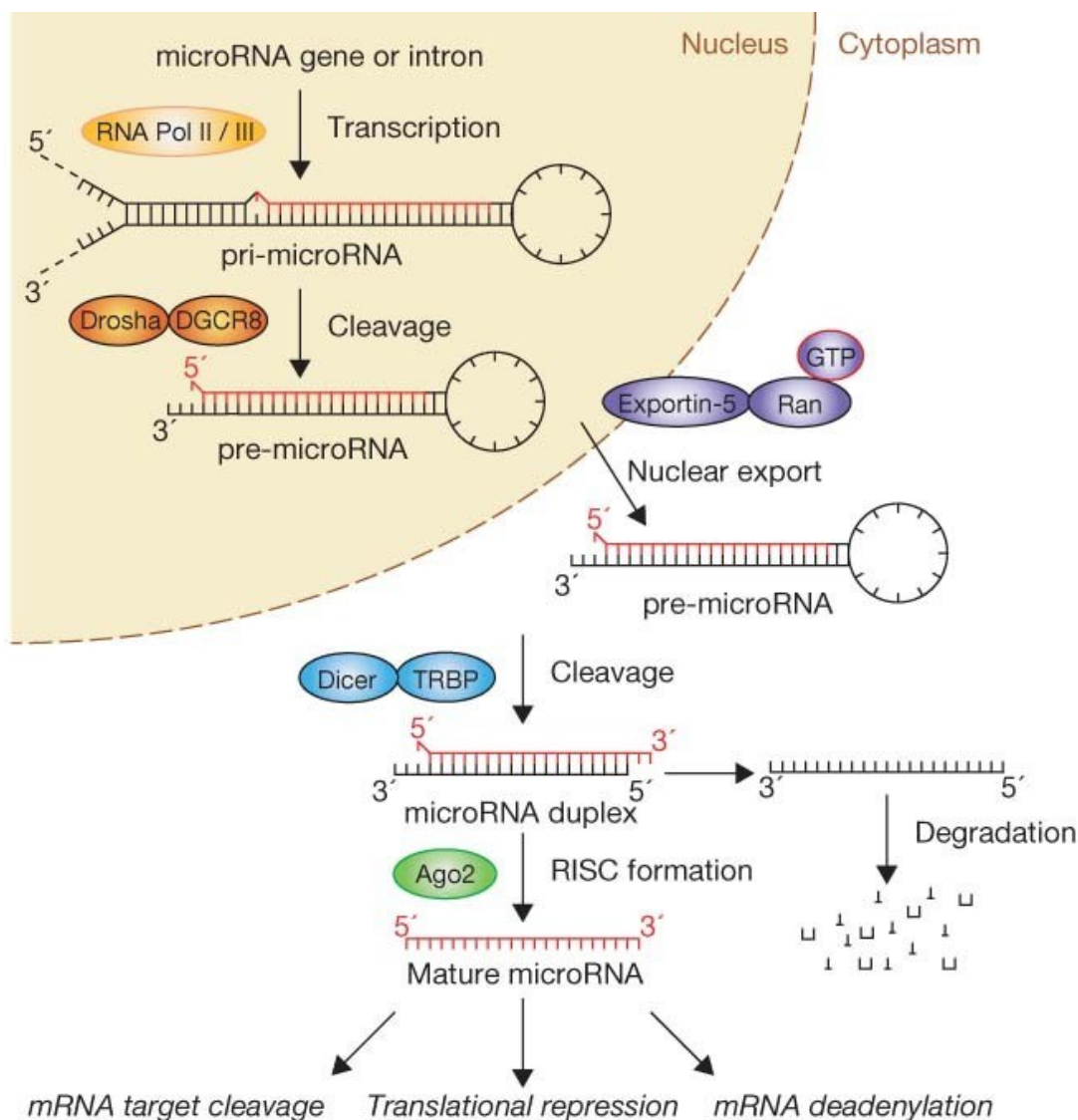


Fig. 2 Biogenesis of miRNA. Canonical processing pathway of miRNAs starts in nucleus, firstly there is primary miRNA (pri-miRNA), after cleavage by Drosha-DGCR8 complex pre-miRNA is formed and later exported to cytoplasm and cleaved further until the mature miRNA is formed. (Figure adapted from (Winter et al., 2009)

1.2.3 Mechanism of function

Further is described the mechanism of miRNA function only in animals, not plants (there is a different mechanism of miRNAs action). Binding of miRNA in RISC (miRISC) is important for specific recognition of target mRNA. Generally, miRNA-binding sites are set in 3'UTR (untranslated region) of mRNA in multiple copies. MiRNA is bound to these sites by Watson-Crick base pairing in length of 2-8 nucleotides – which is called as seed region. According to the level of miRNA-mRNA complementarity the way of suppressing the gene is chosen – perfect complementarity allows cleavage of the mRNA strand. If central mismatches occur, cleavage does not happen, but the translation of mRNA is repressed. Guo et al. found out, that inhibition of translation had just slight effect compared to destabilization of mRNA (Guo et al., 2010). It is unclear if the repression occurs in initiation of translation or in the later phase. There are three models of possible repression by miRISC, the first is competition of miRISC and eIF4E for binding to 5' cap structure. The second is deadenylation, therefore destabilizing the mRNA, and the third is miRISC blocks the association of large and small ribosomal subunits (Chendrimada et al., 2007). MiRNAs can also act as transcription activators by binding to enhancer sequences (Xiao et al., 2016).

1.2.4 MiR-155 expression in hematopoietic cells

The sequence coding mature miR-155 is highly conserved in humans, mice and chickens (Mashima, 2015), MiR-155 physiologically involves in the lymphoid and myeloid cells development where the levels of miR-155 differ depending on the cell type (Georgantas et al., 2007). During the erythroid differentiation *in vitro*, there was proven, that the level of miR-155 was 200 fold lower in mature red cells, and miR-451 was upregulated at the same time. Demonstrating, that these two miRNAs are crucial for differentiation in myelopoiesis and erythropoiesis (Georgantas et al., 2007).

One of the roles of miR-155 is maturation of B-cell and T-cell. MiR-155 is known as oncomir to many types of leukemias/cancers, such as Hodgkin Lymphoma and subtypes of Non-Hodgkin lymphomas, lung cancer, breast cancer and many others (Eis et al., 2005; Kluiver et al., 2005; Wang et al., 2016; Yi et al., 2018). MiR-155 is also involved in inflammatory pathways. The B-cell development is directly affected by transcriptional factors, which are connected to miRNAs. Deregulated expression of miRNAs and transcription factors are key events in pathogenesis of B-cell malignancies (Fabbri & Croce, 2011). In physiological lymphopoiesis, the highest level of miR-155 is expressed in germinal center cells, intermediate

level hematopoietic stem cells and the lowest mature B-cells (Georgantas et al., 2007). It has been reported that direct target of miR-155 is *SHIP1* (Src homology-2 domain-containing inositol 5-phosphatase 1) gene that regulates differentiation of B, T-cells and macrophages (O'Connell et al., 2011).

There are two types of B-cell activation: T-independent and T-dependent B-cell activation. In the first case, as the name says, it's independent of T-cells. Binding of BCR (B-cell receptor) clusters triggers B-cell activation. The accessory proteins like $Ig\alpha$ or $Ig\beta$ on the B-cell surface. The antigen-binding signal is then conveyed to the nucleus. The first signal is thanks to BCR, the second one is made by binding of the toll-like receptor to the antigen. After this, the B-cell turns into a plasma cell and generates IgM antibodies. Memory cells are not produced in this case.

T-independent B-cell activation was a two signal process. On the other hand, T-dependent B-cell activation is a three signal process. The first signal is the same, which is binding of BCR to the antigen. The B-cell processes the antigen and presents part of it on its surface via the MHC II-peptide complex. These B-cells also start to present co-stimulatory and cytokine receptors on their surface. The most important one is CD40. The same antigen is also recognized by T helper cells. The second signal takes place between the B-cell and the T helper cell. The binding is thanks to the antigen on the surface of the B-cell and the CD40 receptor being bound to the CD40 ligand. After that, the T helper cell releases cytokines, which stimulate the B-cell, which expresses cytokine receptors on its surface. The T cell releases interleukin 4, which binds to the cytokine receptors. After that, B-cells start to proliferate and differentiate into plasma cells and memory cells.

The level of miR-155 expression is elevated during B-cell maturation in germinal centers, which happens at the beginning of CD40 ligand and receptor binding - the response to T-cells; and also during initiation of proliferation. It was found, that depletion of miR-155 resulted in disruption of these processes (Rodriguez et al., 2007; Thai et al., 2007). MiR-155 also affects cytokine production. In miR-155 depleted cells, TNF production and its transcripts were reduced. In further processes, higher expression of miR-155 was also observed in the immunoglobulin switch process. Cells lacking this miRNA were not able to produce IgG1 antibodies, which resulted in reduction of cells with expression of IgG1 on the surface (Vigorito et al., 2007). The transcription factor PU.1 was established as a direct target of miR-155. PU.1

is directly suppressed by miR-155, which was proven in high expression of PU.1 in miR-155 deficient B-cells (Vigorito et al., 2007). When PU.1 was over-expressed in wild-type B-cells, it resulted in reduced numbers of IgG1-switched cells, indicating that the loss of PU.1 regulation contributes to the observed miR-155-deficient phenotype (Vigorito et al., 2007).

MiR-155 is also crucial for hypermutation, gene conversion and class-switch recombination during activation of B-cells. By affecting AID (activation-induced cytidine deaminase), which converts cytidine residues into uridine residues, leads to single strand nick in the DNA and further to gene conversion and class switch recombination. Control of AID is important for maintaining genomic integrity. It was observed, that miR-155 expression is induced along with AID in activated leukocytes in germinal center B-cells. In miR-155 deficient cells, the level of AID was even higher, that confirmed miR-155 inhibitory role on AID levels (Dorsett et al., 2008; Teng et al., 2008; Vigorito et al., 2007). All these points out on crucial role of miR-155 in post-transcriptional regulation of gene expression in the terminal differentiation of B-cells.

The role of miR-155 in the myeloid compartment

In macrophages and monocytes, the miR-155 level rises in response to lipopolysaccharides (LPS) or interferon (IFN) signaling. Implying, that miR-155 is crucial for the innate immune response to viral or bacterial infections (O'Connell et al., 2007; Tili et al., 2007). As a response to LPS signaling, TNF translation initiation is triggered. It was found, that under certain circumstances, such as this, miRNAs enhance translation (Tili et al., 2007).

The JNK pathway is part of the upregulated expression of miR-155 (O'Connell et al., 2007). Also another pathway which is may be under control of the expression of miR155 is NF- κ B, especially after viral infections, the level of miR-155 is upregulated. This regulation happens through binding of NF- κ B in the *BIC* promoter, which has conserved sited for NF- κ B binding. Otherwise in these cells the rolf of NF- κ B is unclear (Tili et al., 2009).

In T-cells

MiR-155 promotes T_H1 (T helper cell) and also T_H2. Lack of miR-155 resulted in promoting only T_H2 cells (Rodriguez et al., 2007) and producing more of IL-4 and less of IFN- γ . *FOXP3* was shown to bind to an intron within *BIC* (Marson et al., 2007; Zheng & Rudensky,

2007). Foxp3 is in control of expression of miR-155, loss of Foxp3 resulted in loss of miR-155 expression (Gavin et al., 2007; Marson et al., 2007; Zheng & Rudensky, 2007). MiR-155 is required to maintain the proliferative fitness of Treg cells only when they have to compete for limiting amounts of growth factors (Gavin et al., 2007) miR-155 is affecting transcription factors in T-cells such as PU.1 and c-MAF.

There were also findings connecting the infection of primary B lymphocytes by EpsteinBarr virus (EBV). Result of this infection was in sustained elevation of BIC/miR-155 levels (F. Lu et al., 2008; Yin, McBride, et al., 2008). The EBV-encoded latent membrane protein-1, a potent activator of NF- κ B signaling pathways, which is essential for EBV immortalization of B lymphocytes, substantially up-regulated miR-155 when transfected in EBV-negative B-cells (F. Lu et al., 2008). This upregulation was attributed to two putative NF- κ B binding sites in the miR-155 promoter (Gatto et al., 2008). This latent membrane protein-1-mediated activation of miR-155 correlated with a reduction of PU.1 and IKK ϵ levels (Gatto et al., 2008; F. Lu et al., 2008), both targets of miR-155. These reports suggested that miR-155 contributes to EBV immortalization by modulating the NF- κ B signaling pathway and suppressing the host innate immunity to latent viral infection. Another report showed that the induction of miR-155 in EBV infected cells requires the presence of AP-1 binding sites in the miR-155 promoter (Yin, McBride, et al., 2008). In summary, present results suggest that either expressed by the viruses or up-regulated by viral infections, miR-155 contributes to viral-mediated infections in part through the modulation of different transcription factors and the NF- κ B components targeted by both the host miR-155 and the viral-encoded miR-155.

Different levels of expression of miR-155 bring different outputs

High levels of miRNA-155 have been found in many sorts of cancers or leukemias. As oncogenic miRNA its targets are tumor suppressor genes. Levels of miR-155 in tumors compared to normal tissues are lower, than the levels reached during immune response, so it is considerate to think different levels have different outputs. The high levels of miR-155 potentially turn on the Activation-Induced Cell Death pathway, block the activation of cell cycle and target potential oncogenes. In cancer cells miR-155 reaches the intermediate level, resulting in oncogenic effects.

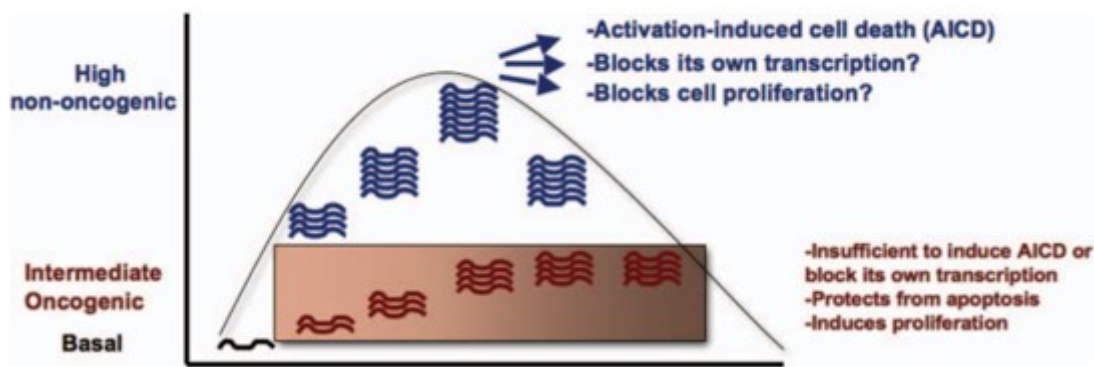


Fig. 3 A working model for miR-155 has many impacts as a function of its concentration. During the immunological response, miR-155 reaches transiently high levels of expression. Although higher than in controls, miR-155 levels in certain malignancies are still low when compared to levels attained during the immune response. High levels of miR-155 have the potential to cause AICD and inhibit cell growth. Furthermore, high amounts of miR-155 may directly or indirectly inhibit BIC/miR-155 transcription. Intermediate levels of miR-155 observed in certain tumors, on the other hand, are unable to carry out any of the above functions and are hence carcinogenic.(adapted from Tili et al., 2009)

Even though miR-155 is affecting number of transcripts, its effect depends on the context of cellular activity. For example, during clonal expansion, some of the transcripts may be absent but present in other conditions in the same cell.

The clonal expansion of immune cells is an important hallmark of the immune response. However, at the end of the immune response, 99 % of lymphocytes are eliminated and just a few resting cells become memory cells. Uncontrolled proliferation is an everlasting/ongoing risk during every immune response. Levels of miR-155 are controlled through TCR (T-cell receptor), BCR (B-cell receptor) or TLR (Toll-like receptor). Arrangement of these simultaneously induced pathways activates the proliferation, but also the elimination of the expanded lymphocytes. It is possible that signals through these receptors lead to different responses according to the time of happening, during the immune response.

Some of the signals originating from BCR, TCR, or TLR engagements may potentially drive miR-155 to target its own transcriptional activators, thus establishing feedback inhibitory loops, keeping the immune response under control while maintaining cell homeostasis. In malignancies, however, elevated levels of miR-155 are probably due to its persistent activation by upstream oncogenes and subsequent escaping of feedback inhibitory loops. It is likely that miR-155 expressed at prolonged intermediate levels may target transcripts that would otherwise not be targeted under high, but transient, miR-155 levels. It is also possible that miR-155 targets

the same transcripts during the immune response or during oncogenesis, but nevertheless, depending on its level of expression, it might not always be able to neutralize the effects of the It seems that the micro-inflammatory environment may be a cause of prolonged miR-155 expression by exhibiting inflammatory signals to macrophages or monocytes. Therefore, affects other blood cells, which reinitiate the up-regulation of miR-155. However, this regulation is slightly increased and accompanied by signals to down regulate it and reach the level which later contributes to developing pre-cancerous cells (Tili et al., 2009).

Slight increase of Myc levels may initiate oncogenesis more efficiently than higher levels of Myc expression (Murphy et al., 2008). The situation with miR-155 may be similar so, as the outcome – different levels of miR-155 have different outputs.

In summary, miR-155 has a broad role in the immune system, and is important for hematopoiesis by modulating the differentiation of B, T, megakaryocytes, erythrocytes and monocytes/macrophages. It also regulates innate and acquired immunity through antibody production, cytokine release or down regulation of different transcription factors. MiR-155 is regulated by inflammatory factors, such as cytokines, TLR, BCR and TCR signaling, in addition to JNK or NF- κ B pathways.

Regulatory role of miR-155 and its targets

The number of target genes according to miRTarBase is 3287 (January, 2021), which supports the fact that miR-155 represents multifunctional miRNA.

The group of Yu et al. found out, that in colorectal carcinome, the miR-155 is responsible for regulating the proliferation, cell cycle, apoptosis and migration of colon cancer cells (Yu et al., 2017). The inhibition of apoptosis by affecting by *PTEN* pathway was confirmed in psoriasis by (Xu et al., 2017). Knockout of miR-155 in mice lead to attenuation of immune system (Vigorito et al., 2013).

The *SHIP1* (Src homology-2 domain-containing inositol 5-phosphatase 1) gene, which affects B, T, and macrophage development, has been identified as a direct target of miR-155 (O'Connell et al., 2011). SHIP1 knockout mice developed germinal centers spontaneously and switched antibody classes (Helgason et al., 2000).

The presence of miR-155 is required for the activation of the B-cell receptor (BCR) during B-cell maturation: crucial for antibody production (Yin, Wang, et al., 2008). B-CLL cells with increased miR-155 expression had a better capability for BCR signaling (Chen et al., 2002, s. 70).

The final step of B-cell development occurs in the peripheral lymphoid organs, where centroblasts and activated B-cells express miR-155, which is required for normal B-cell development (Fernando et al., 2012).

B-cells, T-cells, and common lymphoid, myeloid progenitors all require *MYB* for self-renewal. *MYB* expression is highest in long-term HSCs, and its output decreases as B-cells mature (Greig et al., 2010). *MYB* is required for the transition from pro-B to pre-B cells during early B-cell development (Fahl et al., 2009). *MYB* deficiency causes a partial stop during B-cell development at the pro-B to pre-B cell transition, resulting in a significantly reduced bone marrow generation of new B-cells. In addition, the lack of *MYB* impairs proper B-cell homeostasis by reducing splenic B-cell survival (Thomas et al., 2005). *MYB* is essential for CD19+ pro B-cell survival and accumulation in the peripheral blood (Fahl et al., 2009). The deletion or mutation of *MYB* causes a deficiency in B-cell lymphopoiesis.

Out of these miR-155 targets, only a few are related to B-cell development, cell cycle, differentiation, and CLL pathogenesis. Certain targets (such as *PU.1* and proto-oncogene *MYB* transcription factors) belong to the group of so-called "master regulators" of gene expression in hematopoiesis. *PU.1* controls the process of hematopoietic cells differentiation in a dose-dependent manner (DeKoter & Singh, 2000). In a case of B-cell differentiation, a low level of *PU.1* restrains B-cell production. At a higher level, *PU.1* blocks the differentiation of B-cells into plasma cells (D. Lu et al., 2014; Vigorito et al., 2013). Previously group of Vargova et al. described the direct negative relationship between the elevated level of miR-155 and downregulation of *PU.1* in CLL (Huskova et al., 2015; Pospisil et al., 2011; Vargova et al., 2017). A recent study shows that miR-155 affects mitosis and chromosomal stability during tumorigenesis. The authors described novel targets of miR-155 that interact with cell cycle regulatory proteins. The mechanism of miRNA action on genome stability and ploidy is still described scarcely.

The question of how miRNAs orchestrate the cell fate through their respective targets in CLL remains enigmatic. Answering this question is crucial for the understanding of the molecular network of CLL leukemogenesis.

2. Hypothesis

Imbalance in miRNA expression represents one among many factors that initiate leukemia/cancer. OncomiR-155 is highly expressed in many leukemias/cancers, including CLL. The process of leukemogenesis is associated with changes in the gene expression profile of mRNAs, the miRNAs targets. Elevated levels of miR-155 results in suppression of its targets.

We hypothesize that by gene editing of CLL B-cells we unblock miR-155 targets and find out correlation between these targets (known and also unknown) in CLL during leukemia progression.

2.1 Aims of the thesis

1. Create the miR-155 deficient CLL cell line HG-3 with the use of CRISPR/Cas9 tool.
2. Investigate the influence of miR-155 deficiency on cell viability and proliferation (in HG-3 cell line).
3. Perform qRT-PCR to compare the gene expression profile of HG-3 cells before and after gene editing.

2.2 Specific aims of the thesis

1. What kind of differences we can detect in the transcriptome of CLL cell lines HG-3 and MEC-1 after deletion of mature miR-155 by CRISPR/Cas9 in these cells? (up/down expression of miR-155 validated/novel targets).
2. Compare the proliferation rate of CLL cell lines HG-3 and MEC-1 with/without deletion of mature miR-155 created with the use of CRISPR/Cas9 tool.

3. Material and Methods

In all experiments performed in this thesis, the HG-3 and MEC-1 cell lines were used. HG-3 cell line is derived from a Caucasian man diagnosed with an early stage of Chronic Lymphocytic Leukemia disease. Experiments with MEC-1 cell line were performed earlier by Dr. Savvulidi Vargová

For gene editing, the CRISPR/Cas9 method was used. In all the cell lines mentioned above, we used commercial plasmid (vector) pU6gRNA-Cas9-GFP (#10021426MN, Sigma). Plasmid was generated commercially by providing sequence responsible for mature miR-155, which is 23 bp long „TTAATGCTAATCGTGATAGGGGT“ in *MIR155HG/BIC* gene within the region 5' 25,573,983 to 25,574,004 3' (NC_000021.9 (25573980...25574044), Chr 21, GRCh38.p13). The plasmid map depicted in figure 4 shows parts of plasmid in detail as follow - Cas9 (CRISPR associated protein 9), which performs specific cleavage, binds to DNA by pairing of sgRNA to the target (in future cleaved) DNA; sequence gRNA (guide), which has the same sequence as mature miR-155; GFP (green fluorescence protein) used for identification and resistance against antibiotics (Kanamycin, KanR); pUC ori is the origin of plasmid replication. Plasmid contains Cytomegalovirus (CMV) promoter, and as terminator the bovine growth hormone polyadenylation (bgh-PolyA, BGH pA) signal is used (BGH) and 2A self-cleaving peptides. Plasmid was stored at -20°C and handled by following the manufacturer's protocol.

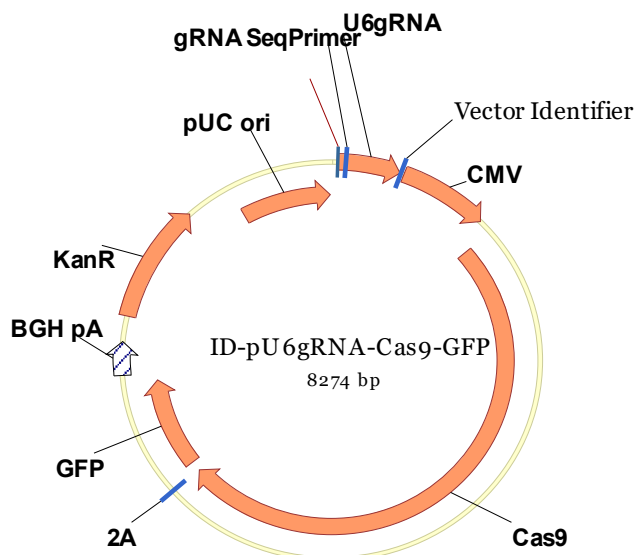


Fig. 4 Plasmid map of expression vector used for CRISPR/Cas9 gene editing - U6gRNA-Cas9-2A-GFP miR-155 (Sigma).

Afterwards the viable cells that contained GFP were selected by Fluorescence-activated cell sorting. Clones of GFP positive HG-3 cells were cultivated for 3 – 4 weeks after nucleofection. After that, cryopreservation, DNA and RNA isolation were performed.

Isolated DNA was multiplied by Polymerase Chain Reaction (PCR), then transferred to 2% Agarose electrophoresis gel. The PCR product of the desired length was isolated from the gel and sequenced (Sanger sequencing) to verify if desired deletion of 22 nt responsible for mature miR-155 was successful.

Isolated RNA of gained clones with deletion of sequence for mature miR-155 was used for Quantitative Reverse Transcription Polymerase Chain Reaction (qRT-PCR). This PCR product – complementary DNA (cDNA) was utilized for measuring the changes in transcriptome. The transcriptome of clones was measured and verified by qPCR.

3.1 Material

3.1.1 Biological material

CD19+ B-cells

Healthy B-cells, used in our experiment as controls, were collected from healthy donors from Institute of Hematology and Blood Transfusion in Prague. The commercially available Rosette Sep kit was used as a method of separating CD19+ B-cells. The method is based on the principle of contacting a sample comprising nucleated cells and red blood cells with an antibody composition that causes immunorosettes of the nucleated cells and red blood cells to form. Immunorosettes are formed by several erythrocytes crosslinking a B-cell enrichment antibody cocktail with undesired cells. Tetramer antibody complexes that recognize CD2, CD3, CD16, CD36, CD56, CD66b, and glycoporphin A on erythrocytes are used to remove immunorosettes. Centrifugation over a density medium Ficoll-Paque PREMIUM pellets the undesired cells with free the erythrocytes. Desired cells are collected as a highly enriched population at the interlayer between the plasma and the Ficoll-Paque PREMIUM density medium, without being tagged with the antibody cocktail.

HG-3 Cell line

HG-3 cell line is derived from a 70year old Caucasian man diagnosed with an early stage of Chronic Lymphocytic Leukemia disease (Rai stage II). HG-3 cell line was obtained from DSMZ (Deutsche Sammlung von Mikroorganismen und Zellkulturen – German Collection of

Microorganisms and Cell Cultures). Morphology of HG-3 cells is described as round suspension cells partly growing in clumps and slightly adherent. Its doubling time is between 50 and 60 hours. The immunology profile is negative in these clusters of differentiation: CD3, CD4, CD10, CD13, CD34; positive in these: CD5, CD15, CD19, CD20, CD37, CD80; HLA⁻, DR⁺, cyIgG⁻, cyIgM⁺, cyκ⁻, cyλ⁺.

The karyotype is near-diploid: 46(44-46)<2n>XY, der(10)t(10;11)(q26;q24.1), del(13)(q12q32), there is marginal resemblance to original karyotype. The karyotype consists of 44-46 chromosomes including XY chromosomes, derivative chromosome 10 consisting of q26 part of 10th chromosome and q24.1 part of 11th chromosome; deletion of the 13th chromosome is present between q12 and q32 part of the chromosome.

MEC-1 cell line

MEC-1 cell line was established in 1993 from the peripheral blood of a 61-year-old Caucasian man with chronic B cell leukemia (B-CLL in prolymphocytoid transformation to B-PLL. HG-3 cell line was obtained from DSMZ (Deutsche Sammlung von Mikroorganismen und Zellkulturen – German Collection of Microorganisms and Cell Cultures). Morphology of MEC-1 cells is described as round to polymorphic cells growing in suspension, singly or partly in small aggregates, a few cells are slightly adherent. Its doubling time is around 40 hours. The immunology profile is as follows: CD3⁻, CD10⁻, CD13⁻, CD19⁺, CD20⁺, CD34⁻, CD37⁺, CD38⁺, cyCD79a⁺, CD80⁺, CD138⁺, HLA-DR⁺.

The karyotype is near-diploid with 10% polyploidy - 46(44-47)<2n>XY, -2, +7, -12, +1-2mar, t(1;6)(q22-23;p21), add(7)(q11), der(10)(10pter -> q22::?:2q11->qter), del(17)(p11) - small acf/mar present in most cells - resembles published karyotype.

3.1.2 Chemicals and buffers

Dimethylsulfoxid(DMSO)	Sigma-Aldrich
Fetal Bovine Serum (FBS)	Biosera
Isopropylalkohol p.a.	Sigma-Aldrich
Penicilin-Streptomycin (100x)	Sigma-Aldrich
Phosphate Buffered Saline (PBS) (10x)	Biosera
Propidium iodid (PI)	Sigma-Aldrich
RPMI 1640 medium	Biosera
TRI reagent	iBioTech
plasmid U6gRNA-Cas9-2A-GFP MiR155	Sigma-Aldrich
GeneRuler 100 bp Plus DNA Ladder	Thermo Scientific

Commercial kits

Amaya™ Human B Cell Nucleofector™ Kit	Lonza
DNeasy Blood & Tissue kit	Qiagen
QIAEX II® Gel Extraction Kit	Qiagen
TaqMan Universal PCR Master Mix	Thermo Fisher Scientific

Plasmids

Plasmid which was used for CRISPR/Cas9 reaction is U6gRNA-Cas9-2A-GFP MiR155. The original amount was inserted in *E.coli* and isolated in higher amount later.

3.1.3 Instruments

Amaya nucleofector Device II	Lonza
BD FACS Aria IIu cell sorter	BD Biosciences
BD FACS Canto II fluorescence analyser	BD Biosciences
Bioanalyzer 2100	Agilent Technologies
iBlot Gel Transfer System	Life Technologies
Mastercycler Gradient	Eppendorf
7900HT Fast Real-time PCR System	Life Technologies
ChemiDoc™ Imaging System	

3.2 Methods

3.2.1 Cultivation of HG-3 cell line

HG-3 cell line was cultivated in medium made out of RPMI, 10 % of FBS and 1 % of antibiotics – penicilin/streptomycin. The temperature was 37°C and concentration of CO₂ 5%. Concentration of the cells was between 0,5-1 million cells per mililiter. Culture medium was changed every 2 – 3 days.

Transfection of HG-3 Cells by Amaxa nucleofector

Procedure/method

One day prior nucleofection

1. Firstly the cell number was determined. For one nucleofection reaction 2×10^6 cells was used.
2. Cells were cultured in RPMI medium supplemented with 10 % of FBS, without P/S, 24 hours prior nucleofection. For each well 2 ml of this complete medium was used.
3. Cells were cultured in humidified incubator with 5 % CO₂ and 37°C.

Day of nucleofection

1. Plasmids which were used:
 - a. GFP (pMAX GFP, Amaxa nucleofection kit) c = 0,5 µg/µl as positive control; 2 µg per reaction
 - b. CRISPR/Cas9/miR-155 c = 1 µg per reaction
 - c. CRISPR/Cas9/miR-155 c = 2 µg per reaction
2. Nucleofection solution was prepared. For each reaction 100 µl of complete nucleofection solution was used. Complete nucleofection solution was mixed in ratio of solution:supplement 4,5:1. Nucleofection solution was kept in room temperature in laminar hood.
3. Prepared RPMI medium (without P/S) was preheated at 37°C and divided in 6 well plate; 2 ml of medium per well.
4. Cells were spinned down in eppendorf tubes for 5 minutes, in room temperature with velocity 1900 rpm (300 ref). Supernatant was discarded and the cell pellets were kept on ice.
5. For nucleofection of HG-3 cells by Amaxa nucleofector, nucleofection kit #VPA-1001 and program U-015 were used.

3.2.2 FACS – Fluorescence Activated Cell Sorting and Gaining of the Clones

24 hours after nucleofection desired cells were sorted out by flow cytometry (FACS ARIA II, BD FACSDiva 8.0.1). By sterile single-cell sorting only GFP positive (wavelength 510 nm) and propidium iodid negative (wavelength 617 nm) cells were sorted out in 96 well plate (Fig. 5).

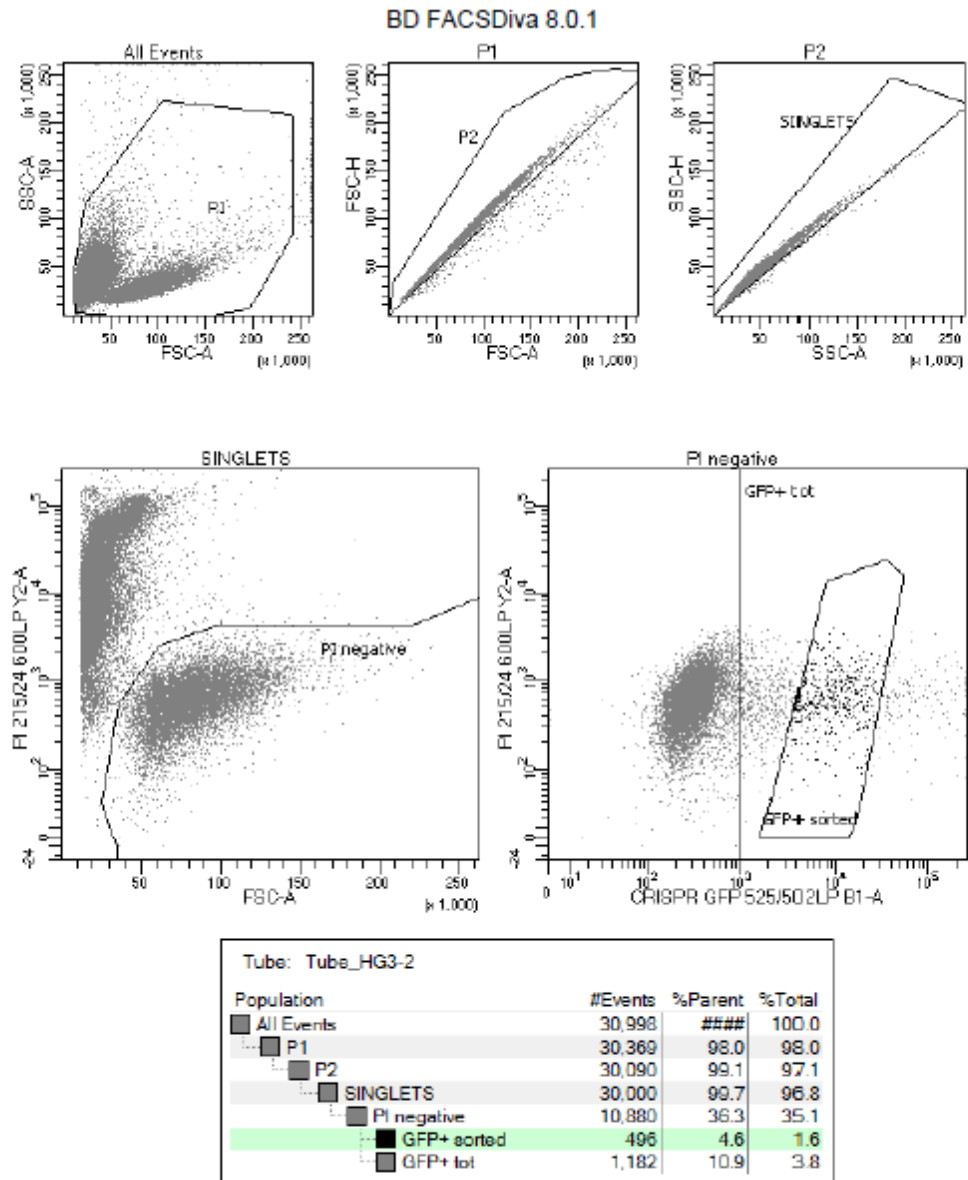


Fig. 5 Presentation of performed FACS sorting.

Sorted single-cells were cultivated in RPMI medium supplemented with 10 % FBS and 1% P/S in humidified incubator with 5 % CO₂. The single cell clones were harvested (after 3-4 weeks of culturing) when the cells reached density around 500 000 cells per milliliter to perform DNA and RNA isolation.

3.2.3 Sequencing

Sanger sequencing was performed in BIOCEV facility.

DNA Isolation

DNeasy Blood & Tissue Qiagen kit for DNA isolation was used and followed the manufacturer's protocol: Purification of Total DNA from Animal Blood or Cells (Spin-Column Protocol) with some modifications.

Protocol for cultured cells was followed and the amount of 5×10^6 cells was used. Firstly the cells were cleaned by centrifugation at speed 14 000 rpm (20 817 G) in PBS for 5 minutes at room temperature. The supernatant was discarded. Then the instructions were followed. Ethanol (96 %) was used. At step 7 in protocol 100 μ l of nuclease-free water (preheated at 56°C) instead of Buffer AE was added into the spin column. This eppendorf tube with spin column was left for 5 minutes at room temperature, spinned down for 1 minute at 8 000 rpm (6797 G), at room temperature. Concentration of DNA was measured by Nanodrop spectrophotometer. The gained DNA was stored at 4°C for short term and at -20°C for long term.

PCR reaction – preparation of product for Sanger Sequencing

Isolated DNA from the previous step was multiplied by Polymerase chain reaction. Because this PCR product was later needed for sequencing, AccuTaq™ LA DNA Polymerase was used. The protocol below for the PCR was pursued. The quantity of gDNA was 100 ng, which differed in the volume of μ l, according to the concentration of DNA in the isolated solution. Altogether the amount for H₂O and DNA solution was 11.8 μ l. For gaining aspecific sequence of mature miR-155 with the length of 358 bp, unique primers were designed (Vector NTI software).

The sequences of primers were following:

Primers	Sequence	Tm
Forward primer	CTCCAGCTTTATAACCGCATCTGC	58°C
Reverse primer	GTTGAACATCCCAGTGACCA	50°C

Accutaq LA 10x buffer	2.0
dNTPs (2.5 mM each, final 10mM)	4.0
DMSO (final c=2%)	0.4
primer F+R 10uM PCR/Seq	1.6
Accutaq LA 10x polymerase	0.2
H ₂ O (nuclease-free)	10.8
gDNA (100 ng/μl)	1.0
<hr/> Total	<hr/> 20.0

Whole reaction mixture consisted of following components:

Reaction: _____ 1x

Program of the reaction was following:

<u>Program:</u>	98°C	30 sec	} 35 cycles
	94°C	10 sec	
	60°C	20 sec	
	68°C	1 min	
	60°C	10 min	
	4°C	1 min	
	4°C	hold	

Gel electrophoresis

For gel electrophoresis 2 % agarose gel was used. Gel was prepared with TBE solution and 2.5 μl of ethidium bromide was added per 50 ml of gel. Loading dye was diluted 6 times in PCR product and this mixture was loaded on agarose gel (20 μL/lane). Electrophoresis lasted one and half hour, with 80 V. For detection of PCR product size DNA ladder 100 bp was used.

Detection of PCR product

Runned agarose gel was viewed by ChemiDoc™ Imaging System to check the size of PCR product. Desired band with proper size of PCR product was cutted out from gel under UV light. Afterward DNA was isolated by gel extracation kit.

DNA extraction from gel

For DNA extraction of desired length from gel commercial QIAEX II® Gel Extraction kit was used. The manufacturer's protocol only with small modification was carefully followed. Modification was done in 9th step where instead of TE buffer the preheated at 56°C nuclease-free water was used.

Gene expression

RNA Isolation

Before starting the RNA Isolation all of the surface and pipettes were cleaned by Nuclease Eliminator solution.

- 1) Cells were harvested, until the amount of 5×10^6 cells was reached. This amount was centrifuged for 5 minutes at room temperature.
- 2) Pellet was resuspended in TRI reagent and left for 5 minutes to complete cell lysis, on bench at room temperature.
- 3) To the TRI reagent cell suspension 100 μ l of chloroform (CHCl_3) was added. This was mixed by vortexing for 2 seconds and left for another 5 min on the bench. After this, the mixture was centrifuged at 11000 rpm (13552 rcf) for 15 min at 10°C.
- 4) The clear upper phase (~250 μ l) was transferred into a new eppendorf tube and mixed with the same amount of CHCl_3 , vortexed and centrifuged at 11000 rpm for 7 min at 10°C.
- 5) The clear upper phase was transferred into new eppendorf tube and 1 μ l of linear acrylamid, 250 μ l of Isopropanol was added. This was vortexed, shortly spinned and precipitated at -20 °C overnight.
- 6) The other day the tube was shortly vortexed and centrifuged at 14000 rpm for 30 min at 4 °C.
- 7) The supernatant was decanted, to the pelet 500 μ l of 75 % ethanol was added, vortexed gently and centrifuged at 14000 rpm for 5 min at 4 °C.
- 8) Supernatant was again decanted, mixture was spinned down shortly and removed rest of the liquid completely, left the pellet to dry on the air for 3-5 min covered with a paper towel.
- 9) The RNA pellet was in 12 μ l of nuclease free water with RNase inhibitors (1 %) dissolved and analyzed by Nanodrop.

The RNA was stored at -80°C .

cDNA synthesis (RT-PCR – reverse transcriptase polymerase chain reaction)

For cDNA synthesis RT Kit was used with reaction mixture below:

<u>Reaction:</u>	1x (μl)
10x RT buffer	1.50
25x dNTPs (100 mM)	0.15
RNase Inhibitors	0.10
RT Random primers	0.25
5x primer miR	1.50
H ₂ O (nuclease-free)	6.50
Reverse transcriptase (RT)	1.00
RNA (100 ng/ μl)	1.00
<hr/>	
total	15.0

Program for reaction was following:

<u>Program:</u>	16 $^{\circ}\text{C}$	30 min
	42 $^{\circ}\text{C}$	30 min
	85 $^{\circ}\text{C}$	5 min

After run of whole program 35 μl of nuclease-free water was added to reach the final amount of 50 μl .

qPCR – quantitative polymerase chain reaction

Mixture for qPCR reaction consisted of 2 fractions – DNA Master Mix and Primer Master Mix. Final volume of PCR reaction was 8 μl in total.

DNA Master Mix:	1x (μl)
TaqMan (Universal PCR Master Mix, cat. nr. 4324018)	2.0
H ₂ O (nuclease-free)	1.5
cDNA	0.5
<hr/>	
total	4.0

Primer Master Mix:	1x (μl)
TaqMan (Universal PCR Master Mix, cat. nr. 4324018)	2.0

Primer (20 μ M)	0.4
Probe (10 μ M)	0.1
H ₂ O (nuclease-free)	1.5
total	4.0

miRNA Master Mix	1x (μ l)
Taq	2.0
20x miR primer	0.4
H ₂ O (nuclease-free)	1.6
total	4.0

There were two separate mixtures for primers, one was for coding genes with specific probes for each gene; the other one for miRNA genes. Firstly 4 μ l of Primer Master Mix were pipetted in 384 well plate, after that 4 μ l of DNA Master Mix.

The reaction was performed by real time PCR instrument (HT7900, ABI) and with following program.

Program		40 cycles
95°C	15 s	
60°C	1 min	

3.2.4 Statistical analysis

All data are presented as mean values \pm standard deviation (SD). In analysis of cell growth (Fig.11,12) data represent the mean of 2 independent experiments (+/-STDEVA). Unpaired, two tailed t-test was used, with statistical significance $p < 0.05$.

The expression of mRNAs/miRNAs in Fig. (15,16) was determined by TaqMan chemistry, analysed by $2^{-\Delta\Delta Ct}$ method (Livak & Schmittgen, 2001). Data from 3 independent experiments are shown as MEDIAN (N=4) compared to controls (healthy B cells) by one way ANOVA with post hoc Dunnett's test (GraphPad software) was used, with statistical significance * $p < 0.05$; ** $p < 0.005$; *** $p < 0.0005$.

In Fig. 17 the expression of mRNAs/miRNAs was determined by TaqMan chemistry, analysed by $2^{-\Delta\Delta Ct}$ method (Livak KJ et al,2001). Data are from 3 independent experiments. Control, gene expression of cells without gene editing, MEC-1 and HG-3 wt cell lines, was set to 1 (white bar, black interrupted line). Unpaired, two tailed t-test was used, with statistical significance * $p < 0.05$; ** $p < 0.005$; *** $p < 0.0005$.

4. Results

Leukemia and cancer development are highly connected to cell cycle and its pathways. Any slight change can have huge impact on future development of the cell (Vermeulen et al. 2003; Ghelli Luserna di Rorà et al. 2019). Small non-coding RNAs have much bigger impact on changing the expression of genes, than was earlier assumed. In this thesis we focused on studying the impact of miR-155 on two cell lines of Chronic Lymphocytic Leukemia. Workflow of experiments performed in thesis depicts

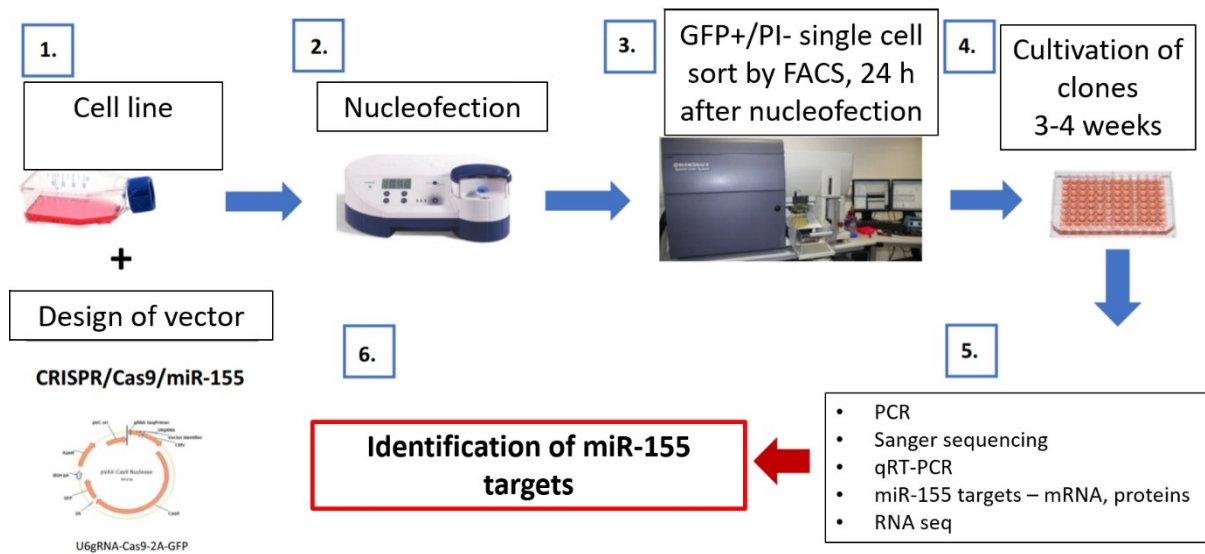


Fig. 6 Workflow of performed experiment. 1. Firstly there was cell line nucleofected with plasmid containing genes for CRISPR/Cas9 editing of miR-155. 2. Nucleofection was performed by AMAXA Nucleofector. 3. GFP+ and PI- cells were selected for further experiments by FACS. 4. Cultivation of selected clones lasted about 3-4 weeks, until gaining sufficient amount of cells for DNA and RNA isolation. 5. Experiments, such as PCR, Sanger sequencing – for confirmation of success rate in deleting of target region, qRT-PCR – for measuring the expression of target genes in gained clones and identifying the miR-155 targets were performed.

Here we focused on the leukemic HG-3 (shown in 9) and MEC-1 cell lines.

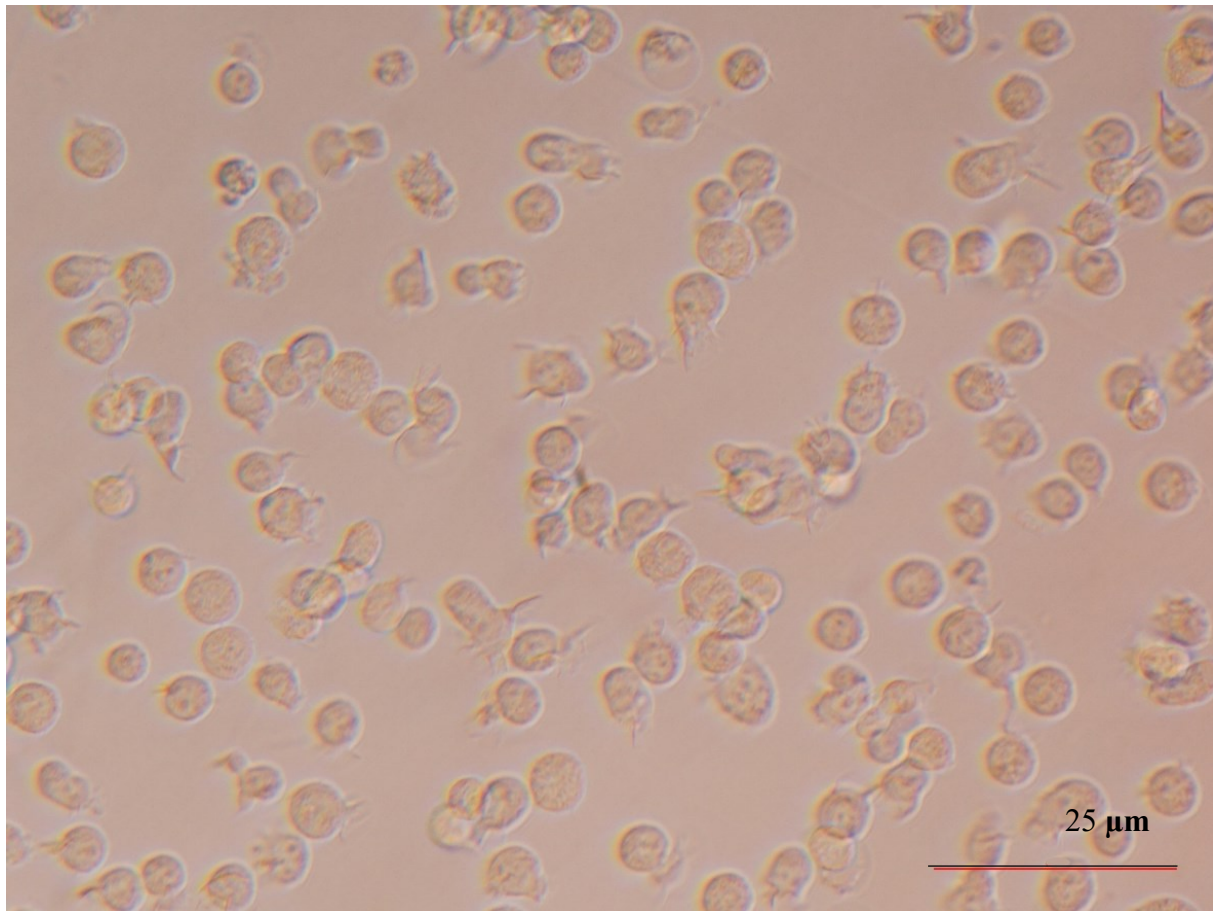


Fig. 7 HG-3 cell line (native). It is stable CLL cell line that consists of kvazi-mature B-cells growing in suspension. Magnification is 200x; one cell is around 5-10 μm large. The red line in the picture represents 25 μm .

Editing of the sequence coding for mature miR-155 by gene-editing technology CRISPR/Cas9 was performed in HG-3 cell line, which represents chronic lymphocytic leukemia (CLL) in early stage of progression. Editing of MEC-1 cell line was done in laboratory by others, in this thesis were performed experiments as cell count, cell viability and qRT-PCR. MEC-1 cells represents adverse CLL stage with *TP53* deletion (del17) (p11). For each gained clone of HG-3 cell line we performed separation of PCR product gel electrophoresis followed by Sanger sequencing to check correctness of gene editing. Fig. 8 shows PCR product of single cell clones of HG-3 cell line, #4 is heterozygous with partial deletion in one strand, two bands are visible.

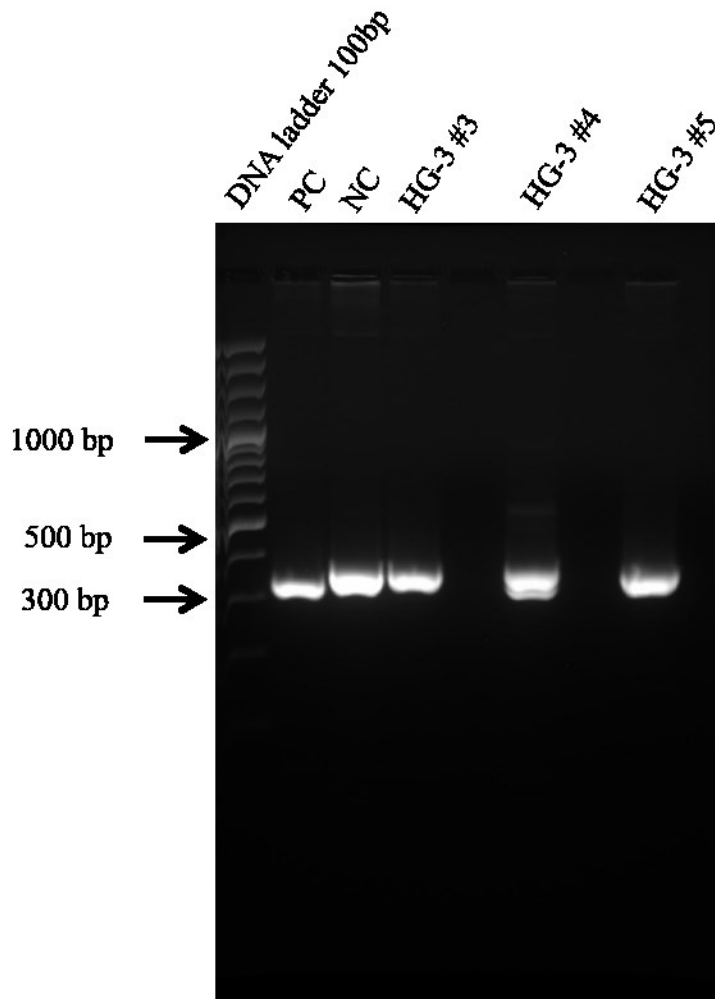


Fig. 8: PCR product of nucleofected HG-3 cell line with CRISPR/Cas9/miR-155 plasmid. Picture depicts different PCR product in CRISPR/Cas9/miR-155 clones isolated from HG-3 cell line. PCR product was separated on 2 % agarose gel, run by 80 V/90 min. Size of PCR product of unedited miR-155 (ctrl) is 358 bp. First column contains DNA ladder 100 bp (#SM0323, ThermoScientific), second column represents positive control - clone #48 with biallelic deletion of miR-155 in MEC-1 cell line, third column represents negative control – wild type of HG-3 cell line (ctrl), fourth column represents clone #3 of HG-3 cell line, fifth column represents clone #4 of HG-3 cell line - containing changes in DNA sequence compared to wild type, two bands are visible, sixth column represents clone #5 of HG-3 cell line.

The model and effectivity of CRISPR/Cas 9 editing is shown in Fig. 9 and 10 for each cell line separately. Using the modern gene-editing technology CRISPR/Cas9 (Fig. 9B, C and D) we have successfully edited the sequence responsible for mature miR-155 at one genomic loci in HG-3 cells. This heterozygous clone #4 bears partially the deletion of the desired sequence, confirmed by Sanger sequencing of the PCR product (Fig. 9E). The same was performed with MEC-1 cell line, with the difference of gaining homozygous clone with deletion at both strands of DNA (Fig.9).

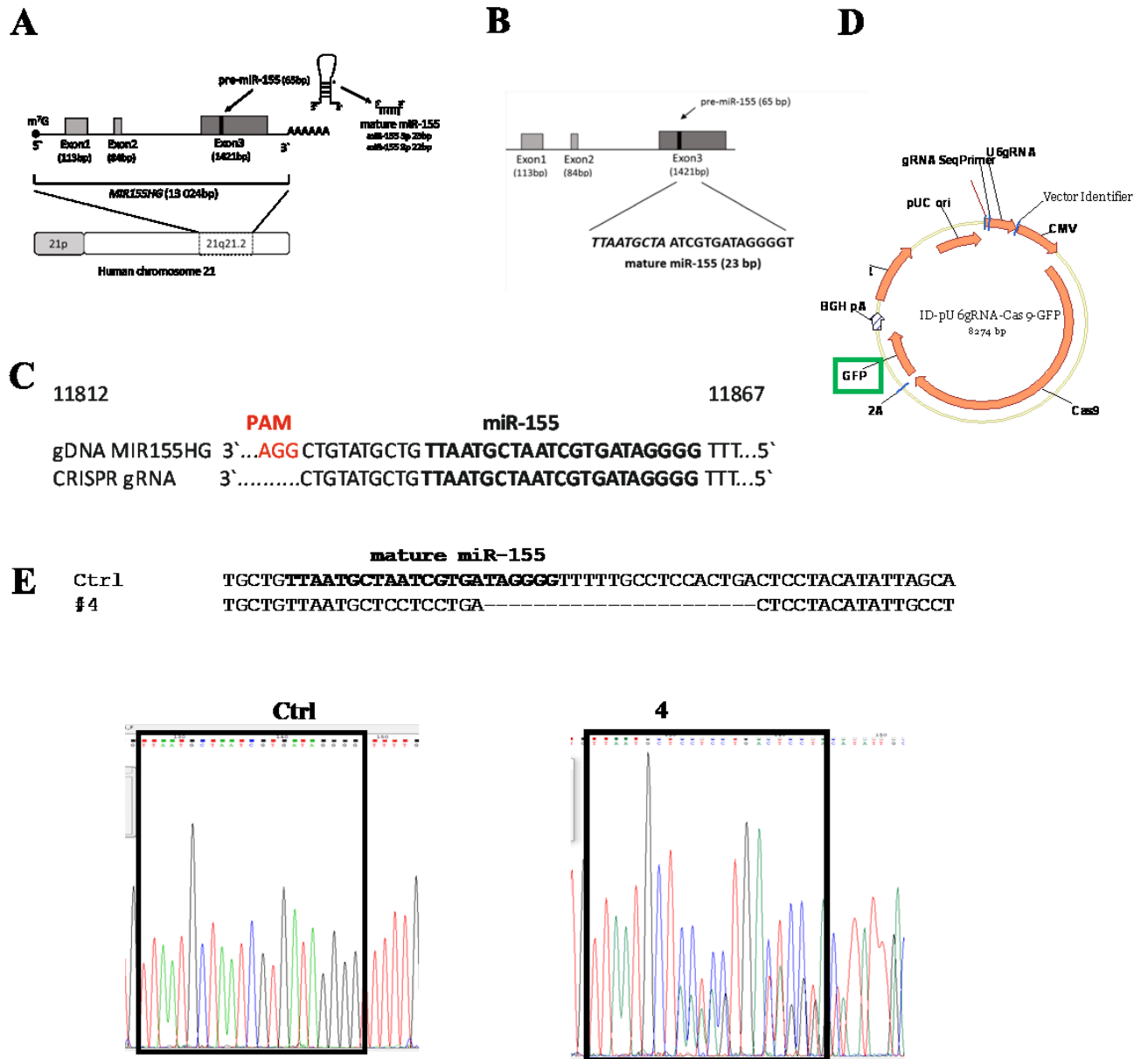


Fig. 9: Schematic illustration of *MIR155HG*, CRISPR/Cas9 miR-155 vector, and deletion of miR-155 in HG-3 cells. (A) Structure of the *MIR155HG/BIC* gene (NC_000021.8). *MIR155HG (BIC)* is localized on the 21q21.2 chromosomal locus. The full length of *MIR155HG* spans 13 024 bp that contains three exons. The exon 3 encodes precursor pre-miR-155 (1421 bp). After two endonuclease cleavage steps (by endonuclease Droscha and Dicer) arises the mature miR-155 (adapted and modified from Tam W, 2001

<http://www.ncbi.nlm.nih.gov/gene/114614>). **(B)** Scheme of *MIR155HG/BIC* gene with depicted and highlighted sequence for mature miR-155 (23 bp). **(C)** The sequence of *MIR155HG* coding mature miR-155 (in bold) and target sequence for gRNA. The PAM sequence AGG in red color. **(D)** Scheme of CRISPR/Cas9/miR-155 vector (pU6gRNA-Cas9-GFP, 8274 bp, Sigma). The vector contains Kanamycin resistance, the sequence for green fluorescence protein (GFP) used as a selection mark. **(E)** The scheme shows the region of *MIR155HG* from 5' 11819 to 11879 3' end, where 21 nt are deleted in case of HG-3 miR-155 deficient clone #4 (heterozygous mutation) in comparison to ctrl (non-edited HG-3 cells). Seed sequence is TAATGCTA. The lower part of the picture shows chromatograms (Sanger sequencing, Chromas software for visualization of pictures were used) of the PCR product in HG-3 cells (ctrl vs #4).

As the cells of miR-155 deficient clones (originating from the single cell) were proliferating slower compared to unedited cells during routine cell culturing, we have decided to follow these observations with advanced approaches. Firstly, we did the standard cell count to assess the cell growth and plot the proliferation curve for both HG-3 and MEC-1 cells (Fig. 11 and 12).

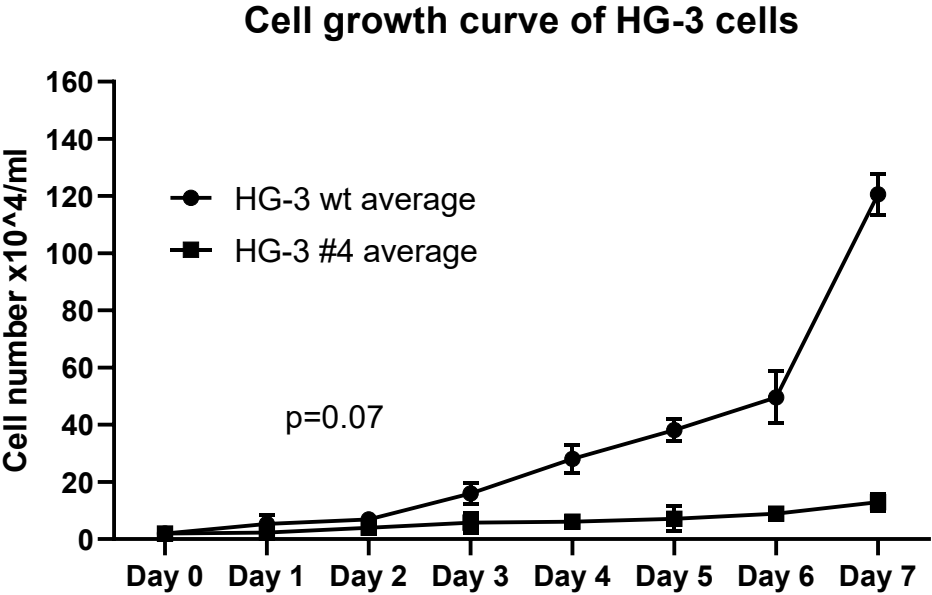


Fig. 11: The proliferation rate of human CLL cell line HG-3. Cell growth curve of HG-3 cells (ctrl - wt and miR-155 deficient clone #4) was determined by cell number count by hemocytometer within 7 days. Seeding density at day 0 was 20 000 cells per well. Y-axis shows cell number and X-axis day. Data represent the mean of 2 independent experiments (+/-STDEVA). Statistics: t-test, two tailed, unpaired was used, $p < 0.05$.

Cell growth curve of MEC-1 cells

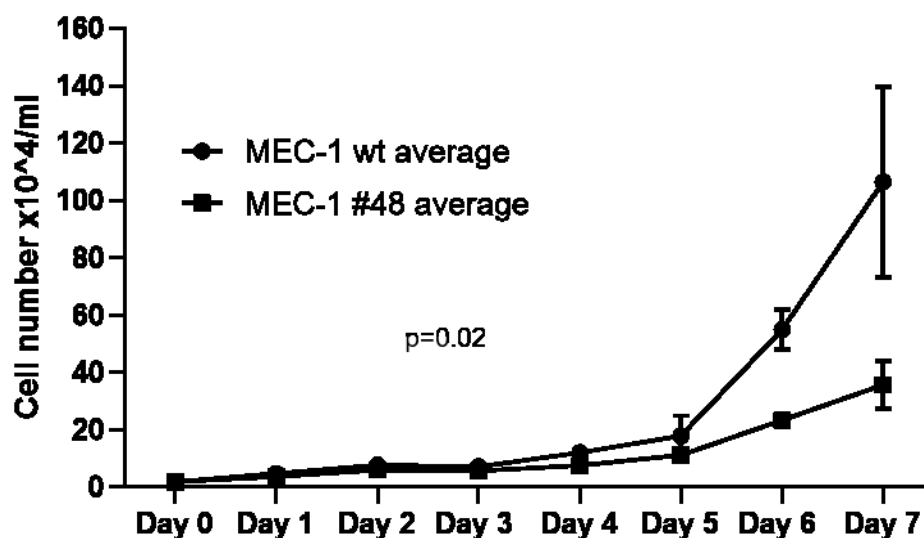


Fig. 12: The proliferation rate of human CLL cell line MEC-1. Cell growth curve of MEC-1 cells (ctrl - wt and miR-155 deficient clone #48) was determined by cell number count by hemocytometer within 7 days. Seeding density at day 0 was 20 000 cells per well. Y-axis shows cell number and X-axis day. Data represent the mean of 2 independent experiments (+/-STDEVA). Statistics: t-test, two tailed, unpaired was used, $p < 0.05$.

In both cell growth curves is significantly visible difference in the level of proliferation speed between wild-type cells and edited clones.

According to this finding, we were curious, if the slower cell growth is connected to higher occurrence of apoptosis or not. Therefore we performed flow cytometry measurement of cells stained with apoptotic protein Annexin V (APC) in period of 7 days. Population of dead cells was detected by propidium iodide. All measurements by flow cytometry are shown in Fig. 13 and 14.

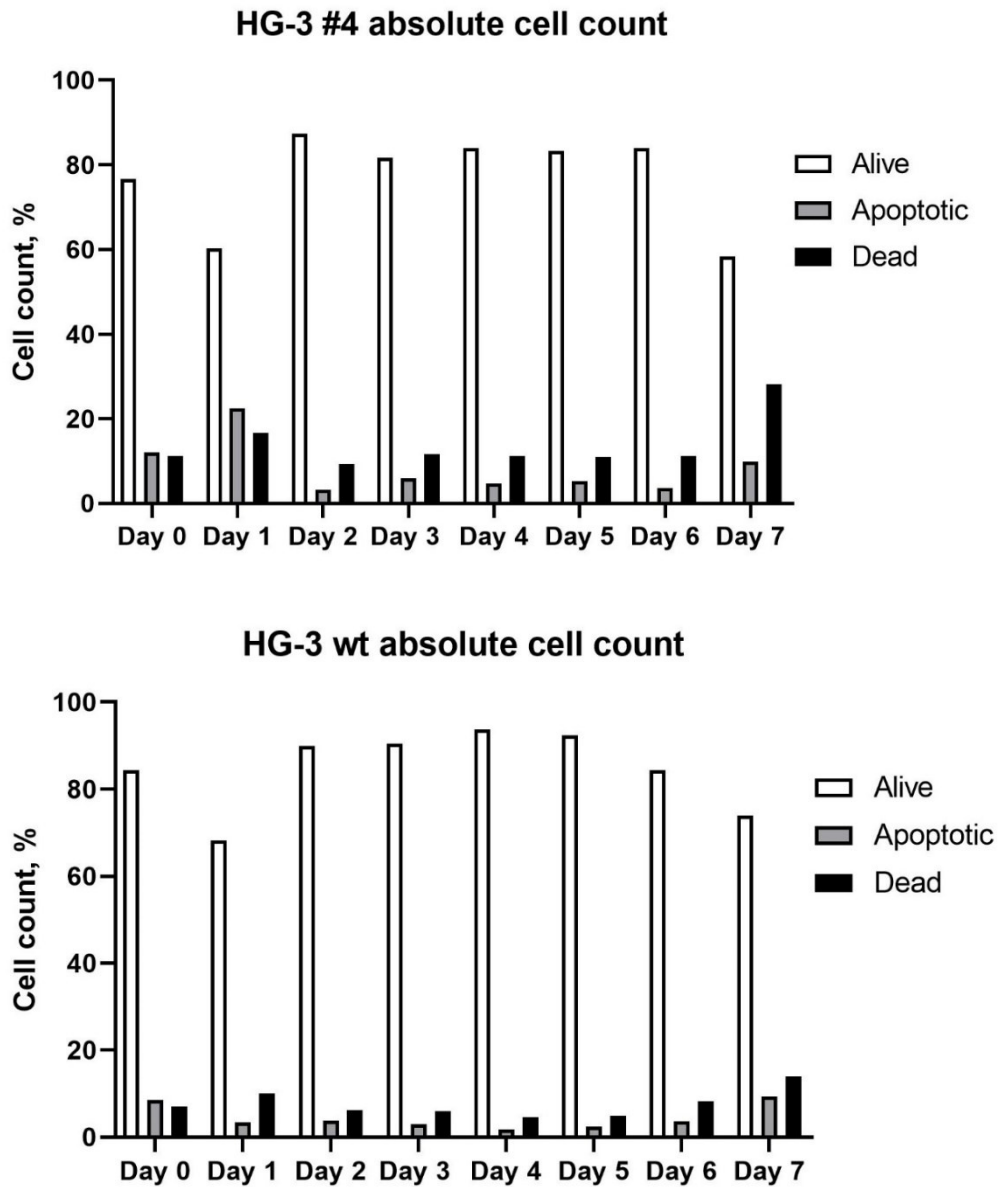


Fig. 13: Viability of HG-3 cells (Evaluation of apoptosis by flow cytometry. HG-3 cells (ctrl and miR-155 deficient clone #4) were stained by *Annexin V/PI* (X-axis, Annexin V, APC, and Y-axis, PI in PE-Cy7 channel). Data were evaluated by Diva software and the measurement was performed with the use of the FACS Canto II BD flow cytometer.

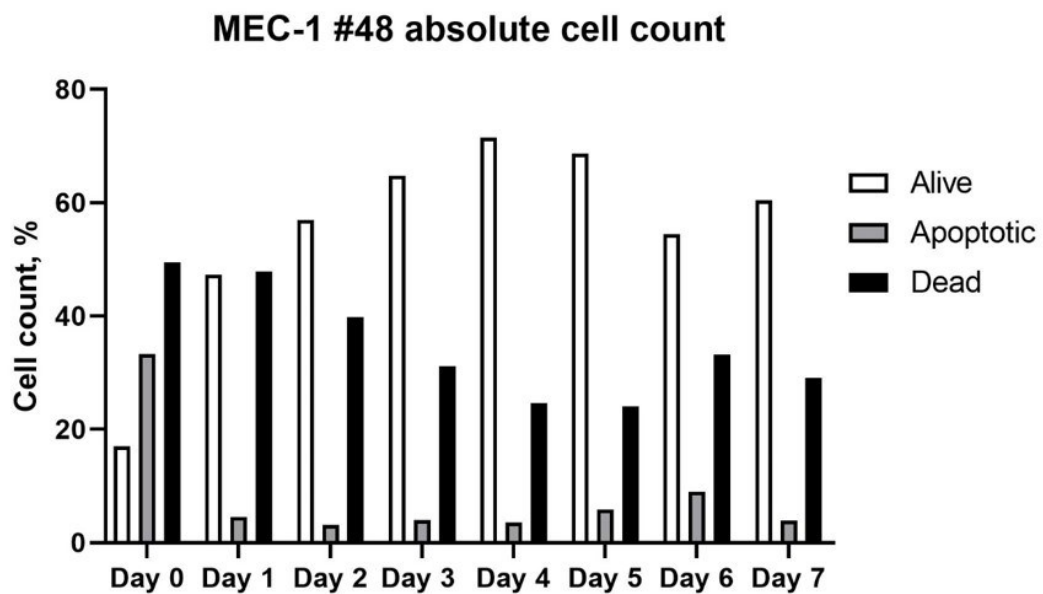
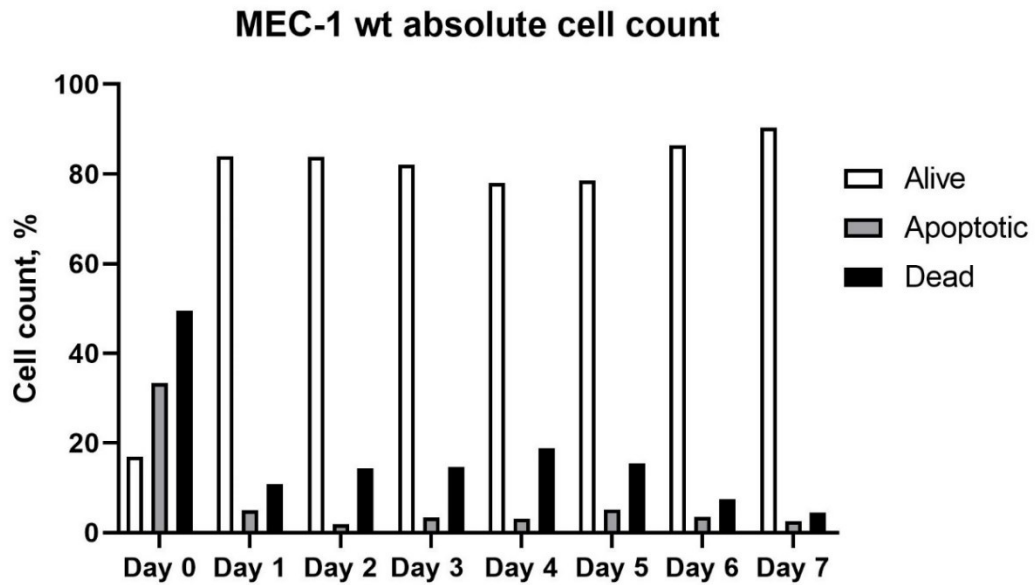


Fig. 14: Viability of MEC-1 cells (Evaluation of apoptosis by flow cytometry. MEC-1 cells (ctrl and miR-155 deficient clone #48) were stained by *Annexin V/PI* (X-axis, Annexin V, APC, and Y-axis, PI in PE-Cy7 channel). Data were evaluated by Diva software and the measurement was performed with the use of the FACS Canto II BD flow cytometer.

As shows Fig. 13 there is practically no difference in the population of apoptotic and dead cells in HG-3 cell line wt vs edited clone #4. Interestingly, MEC-1 cell line shows higher abundance population of dead cells in edited clone #48 in comparison to wild type MEC-1.

In Figures 15, 16, 17 are results of qPCR measurement. In fig. 15 is comparison of HG-3 cell line with healthy B-cells. In fig. 16 is comparison of MEC-1 cell line with healthy B-cells. In fig. 17 are both cell lines, wild type (unedited cell line) of each cell line set at 1 as a control, the expression of other genes is normalized to this value. Following genes (selection of genes was done based on mRNAseq data of MEC-1 cell line) are validated targets of miR-155:

GNB4 – G Protein Subunit Beta 4 gene is located in plasma membrane, coding G protein subunit.

PU.1 – Transcription factor PU.1, located in nucleus which binds to a purine-rich DNA sequence, can act as lymphoid-specific enhancer, this protein is specifically involved in activation and differentiation of macrophages and B-cells. ***PRKAR1A*** - Protein Kinase cAMP-Dependent Type I Regulatory Subunit Alpha, located in plasma membrane and cytosol.

CDKN1A – Cyclin Dependent Kinase Inhibitor 1A is in nucleus and cytosol. This gene encodes a potent cyclin-dependent kinase inhibitor. This specific inhibitor binds to cyclin-cyclin-dependent kinase 2 or 4 complexes, therefore works as regulator of cell cycle in G1 phase.

CDKN2C is an inhibitor of cyclin-dependent kinase, specifically cyclin-dependent kinase 4 and cyclin-dependent kinase 6

FOXP3 is a transcription factor, which is part of regulation of miR-155 in breast cancer. and works as a tumor suppressor in breast and prostate epithelia.

PRKARIA encodes regulatory subunit of the cAMP-dependent protein kinases.

FOS is a gene encoding transcription factor c-Fos and is a protooncogene

MYB is a transcription Factor, proto-oncogene. is a Protein Coding gene.

SHIP1 is phosphatase, which causes the inhibition of the PI3K pathway.

Potential targets are following:

LDHA - Lactate Dehydrogenase A is located in extracellular compartment, cytosol and nucleus. This protein catalyzes the metabolic pathway – converting of L-lactate and NAD to pyruvate and NADH, as last step of anaerobic glycolysis. This protein is more expressed in

cancer and leukemic diseases in order to avoid using mitochondria and cellular respiration cycle as source of energy.

RRP15 - Ribosomal RNA Processing 15 Homolog, located in nucleus, part of protein maturation processes.

RPS29 – Ribosomal Protein S29, located in cytosol, extracellular compartment, nucleus, endoplasmic reticulum, this protein is component of the 40S subunit of ribosomal proteins.

TMSB4X - Thymosin Beta 4 X-Linked, located in cytoskeleton, nucleus and cytosol, actin sequestering protein, plays a role in actin polymerization, this protein is also involved in cell proliferation, migration and differentiation.

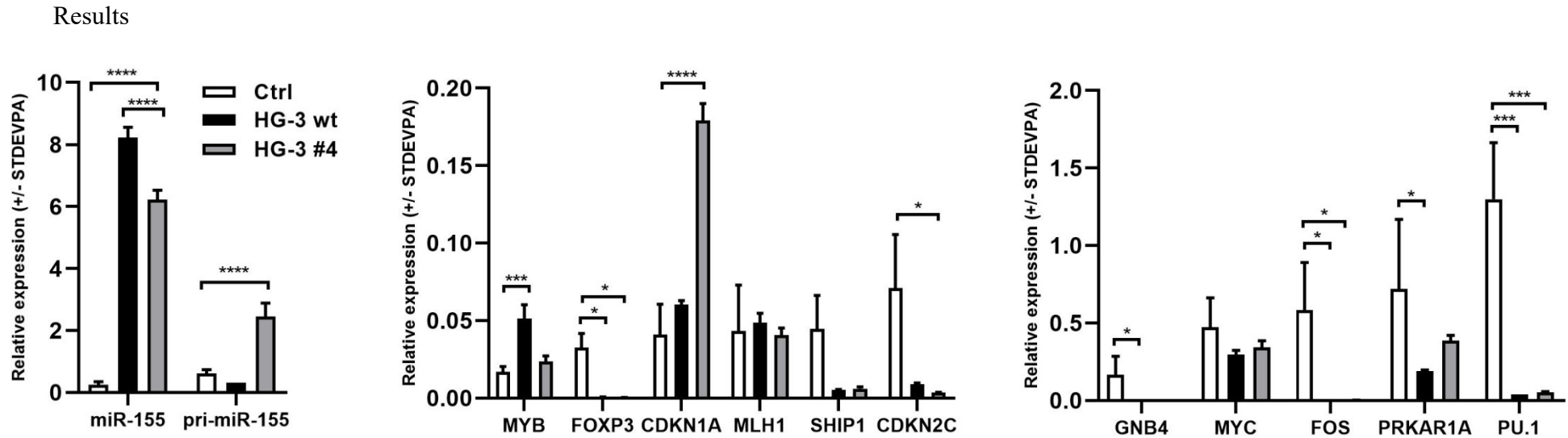
MXI - MX Dynamin Like GTPase 1, located in nucleus and cytosol, this gene encodes protein, which participated in the cellular antiviral response. *ISG15* - ISG15 Ubiquitin Like Modifier, located in extracellular compartment, nucleus and cytosol, this protein functions similarly as ubiquitin.

LMNA - Lamin A/C, located in cytoskeleton, nucleus, cytosol, this protein is part of cytoskeletal proteins.

ISG15 encodes ubiquitin-like protein, which conjugates to intracellular target proteins.

CDK14 encodes cyclin dependent kinase 14, has significant involvement in tumorigenesis.

Validated targets



Predicted targets

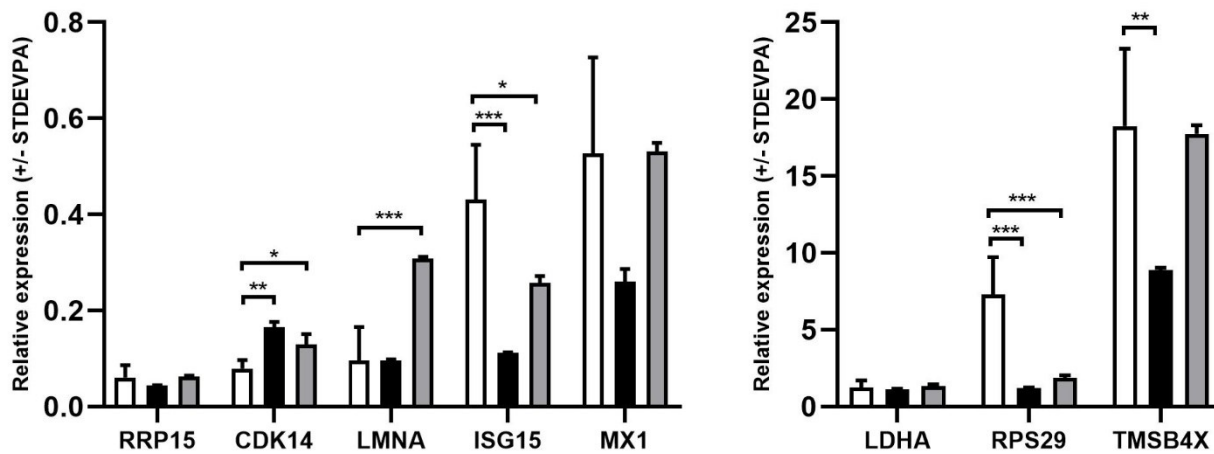


Fig.15: Relative expression of miR-155 targets (validated and predicted; novel CLL related miR-155 targets selected based on the mRNA-seq data) **in HG-3 cell line (wt, clone 4) and in healthy B-cells.** Graphs on the upper part of the figure show relative expression of validated miR-155 targets (based on miRtarBase) in healthy B-cells (obtained from healthy donors, peripheral blood) and HG-3 cell line (wt and clone 4 that bears monoallelic deletion within *MIR155HG*). Ct values of experimental genes were normalized to the reference gene *GAPDH* and in case of miR-155 to *RNU44*. The expression of mRNAs/miRNAs was determined by TaqMan chemistry, analysed by $2^{-\Delta\Delta C_t}$ method (Livak KJ et al, 2001). Data are from 3 independent experiments shown as MEDIAN (N=4), STDEVAPA. Statistics: * $p < 0.05$; ** $p < 0.005$; *** $p < 0.0005$; **** $p < 0.0001$ compared to controls (healthy B cells) by one way ANOVA with post hoc Dunnett's test (GraphPad software) was used.

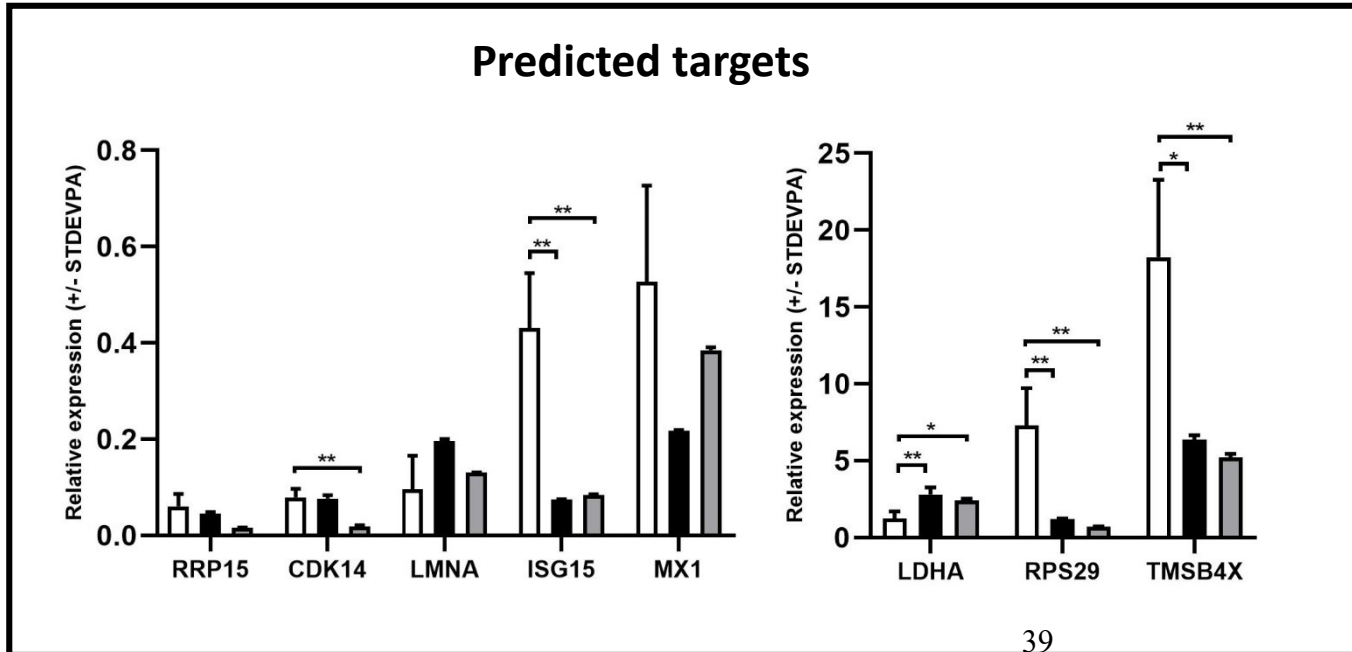
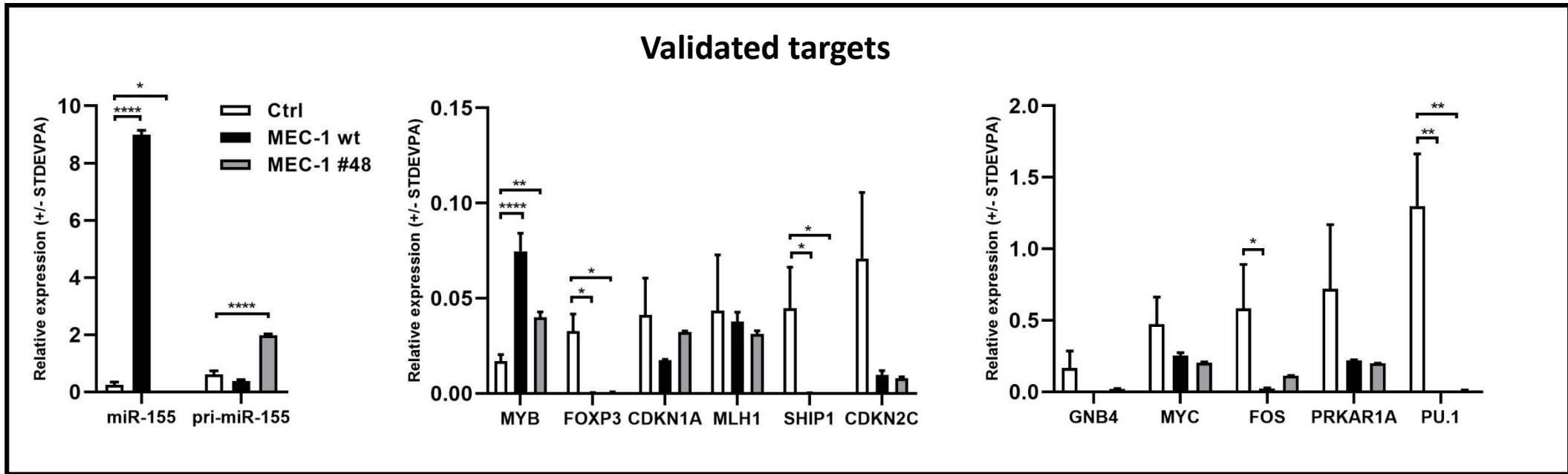
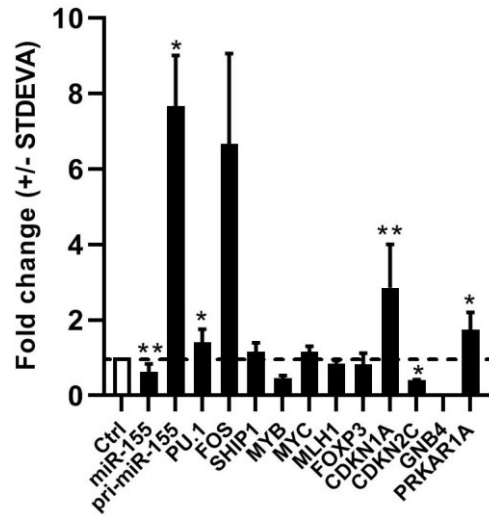
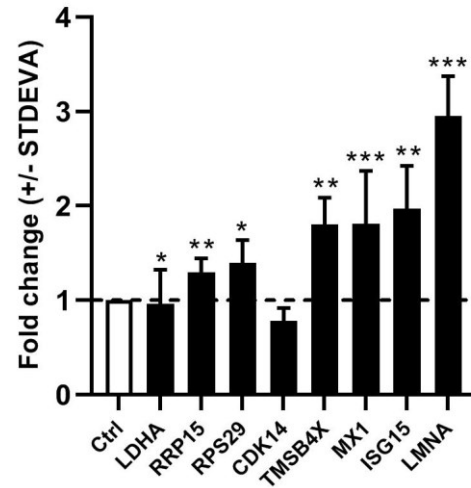


Fig.16 : Relative expression of miR-155 targets (validated and predicted; novel CLL related miR-155 targets selected based on the mRNA-seq data) in MEC-1 cell line (wt, clone 48) and healthy B-cells. Graphs on the upper part of the figure show relative expression of validated miR-155 targets (based on miRtarBase) in healthy B-cells (obtained from healthy donors, peripheral blood) and MEC-1 cell line (wt and clone 48 that bears biallelic deletion within *MIR155HG*). Ct values of experimental genes were normalized to the reference gene *GAPDH* and in case of miR-155 to *RNU44*. The expression of mRNAs/miRNAs was determined by TaqMan chemistry, analysed by $2^{-\Delta\Delta Ct}$ method (Livak KJ et al, 2001). Data are from 3 independent experiments shown as MEDIAN (N=4), STDEVPA. Statistics: *p<0.05; ** p<0.005; *** p<0.0005; **** p<0.0001 compared to controls (healthy B cells) by one way ANOVA with post hoc Dunnett's test (GraphPad software) was used.

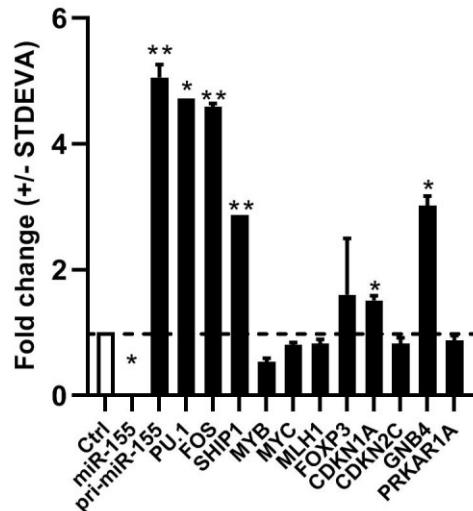
Validated targets of miR-155 in HG-3 #4 cell line



Predicted targets of miR-155 in HG-3 #4 cell line



Validated targets of miR-155 in MEC-1 #48 cell line



Predicted targets of miR-155 in MEC-1 #48 cell line

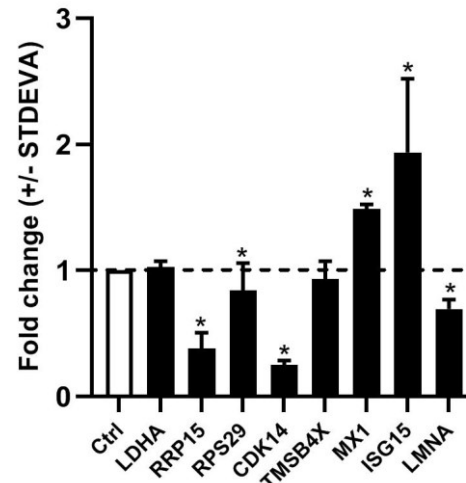


Fig.17: Gene expression profile of miR-155 targets (validated and predicted; novel CLL related miR-155 targets selected based on the mRNA-seq data) **in HG-3 (top) and MEC-1 cell lines** (bottom). Graphs on the upper part of the figure show gene expression (shown as fold change; +/-STDEVA) of HG-3 cell line clone 4 that bears monoallelic deletion within *MIR155HG* in comparison to original HG-3 cell line without gene editing by CRISPR/Cas9. Graphs on the lower part of the figure show gene expression of MEC-1 cell line clone 48 that bears biallelic deletion within *MIR155HG* in comparison to original MEC-1 cell line without gene editing by CRISPR/Cas9. Ct values of experimental genes were normalized to the reference gene *GAPDH* and in case of miR-155 to *RNU44*. The expression of mRNAs/miRNAs was determined by TaqMan chemistry, analysed by $2^{-\Delta\Delta Ct}$ method (Livak KJ et al, 2001). Data are from 3 independent experiments. Ctrl (gene expression of cells without gene editing, MEC-1 and HG-3 wt cell lines) was set to 1 (white bar, black interrupted line). Statistics t-test, two tailed, unpaired was used (* p<0.05; ** p<0.005; *** p<0.0005).

5. Discussion

We worked with two CLL cell lines, both of them with higher expression of miR-155 in comparison to the normal healthy B-cells. HG-3 cell line shows lower expression than MEC-1 that is in concordance with the level of disease stage. We performed nucleofection of these cell lines with plasmid containing all sequences for CRISPR/Cas9 system, gRNA and GFP for detection (for details see Fig.9 D). Gene editing of MEC-1 cell line was performed formerly by Dr. Savvulidi Vargová and the system of gaining mutant cell line remained the same.

By CRISPR/Cas9 tool we created miR-155 deficient mutant of human B-CLL cell line HG-3.

We provided insertion of plasmid by nucleofection, which is electroporation-based transfection method enabling transfer of nucleic acids such as DNA or RNA into cells by applying a specific voltage and reagents. The survival rate of B-cells after nucleofection and flow cytometer cell sorting is generally quite low (Seiffert et al., 2007); we achieved about 1,4 % of cell survival, gaining one clone with changes in DNA sequence. The deletion of miR-155 was partially successful as we gained a clone with deletion of six nucleotides in the coding region of miR-155, positioned on one strand of DNA, therefore heterozygous clone. We assume, that this low efficiency is also caused by the low level of CLL progression in HG-3 cells (intermediate state of CLL), compared to MEC-1 cell line, where the success rate in nucleofection and changing the DNA by CRISPR/Cas9 method was higher (4,3 %). It is known, that with increasing the size of delivered plasmid into cells leads to direct increase of the rate of apoptosis. In our experiments we observed apoptotic rate around 10 % in both CLL cell lines. To avoid technical difficulties, changing of the delivery method may be considered, by lentivirus for example (García-Tuñón et al., 2017). The possibilities of delivering and also editing by CRISPR method are still in process of development of better outcome. Next, to improve the CRISPR/Cas9 gene editing efficiency and to avoid off-target effect we could directly use for nucleofection so called ribonucleoprotein (RNP) complex that consists of Cas9 protein and single guide RNAs (sgRNAs) (Zhang et al., 2021). Also company ThermoFisher Scientific offers commercial kit TrueGuide Synthetic CRISPR gRNA.

In order to identify which nucleotides were deleted by CRISPR/Cas9 we performed Sanger sequencing of PCR product, which showed the deletion in one strand clearly, in the second strand were some changes, but not so clearly identifiable. We would suggest in case of gaining

more clones and choosing the best for further studies, to perform subcloning of PCR product into *E.coli* cells in order to confirm the best fortunate clone.

Exploration of the impact of miR-155 deletion on HG-3 cell line viability and proliferation.

Even though the deletion in HG-3 cell line was just partial in coding sequence of miR-155 and executed in one strand of DNA, the cell growth curve shows, that the number of cells grew with difference between wild type and heterozygous clone. Our results provide support for our research hypothesis. P-value comes up to 0.07, therefore we can't reject the null hypothesis, but the cell growth curve grows significantly higher in seventh day, which is the last day of measurement. If we provided the measurement for longer time, maybe we would record lower p-value. On the other hand, cell growth curve of MEC-1 cell line, has significant difference, as a result we can confirm, that changes in the DNA sequence of miR-155, and deletion of nucleotides lead to slower proliferation of MEC-1 cell line.

Cell viability

We performed measurement of cell viability of both cell lines during 7 days by flow cytometry, focusing on the number of alive, apoptotic and dead cells (Fig. 13,14). Cells were stained by *Annexin V/PI*. The number of HG-3 cells was stable throughout the seven days, about 80 % of cells was alive, the number started to change at the seventh day; any actual difference between control (wild type) and miR-155 heterozygous clone was not detected. These graphs support the data from cell growth curve, that during first six days the number of cells doesn't change much. This can be explained by the moderate level of CLL progression.

MEC-1 cell line showed different outcome, wild type shows high number of alive cells throughout the seven days, quite interestingly, the percentage of alive cells is growing after fifth day. The results from Day 0 we don't include in the observation, because of some propably technical difficulties, since the same trend occurs in both wild type and clone. MEC-1 homozygous clone shows different ratio of alive and dead cells, it may be caused by higher assumption to die because of genetic changes – thanks to CLL, and „curing“ by lack of miR-155, which blocks dying of cells. Or, according to data from the beginning of measurement (Days 1-3), it can be caused by suboptimal defrosting or freezing protocols that led to high amount of dead cells.

Conclusion of cell viability measurements is, that in HG-3 cell line, the viability actually didn't change. In MEC-1 cell line there are changes, but not provided with enough evidence and many factors, which can cause the difference, without any significant influence of the deleting of miR-155. Therefore it would be appropriate to perform this experiment once again to distinguish what caused the difference.

Comparison of the gene expression profile of HG-3 cells before and after gene editing.

We performed qRT-PCR for both CLL cell lines and healthy B-cells, as show Figs.15,16,17. We aligned genes by its expression level. In the first two figures (15,16) we can see the relative expression level in comparison with expression in healthy B-cells. In the third one (17) with the same set of genes ,the gene expression detected in wild type was set as control and set as value 1 to which the other genes were compared. Genes were aligned by Ct (Cycle Threshold) value, firstly validated targets, secondly are shown genes which may be the *bona fide* (potential) targets of miR-155 in CLL.

Significant changes were observed in HG-3 cell line mostly in between the expression of healthy human B-cells, wildtype of HG-3 cell line and also edited monoallelic clone #4 in the expression of *MIR155HG* gene. Eventhough the clone is monoallelic, the expression of miR-155 changed considerably after the CRISPR/Cas9 deletion. Kim *et al.* in their studycompared single vs double knockout cell populations and found out that the loss of miR-155 caused a shift in glucose metabolism via altered regulation of multiple genes involved in glucose usage.

Among the key transcription factor that controls differentiation of hematopoietic cells belongs *PU.1*, also known as SPI1, is an oncogene and also tumor suppressor (DeKoter & Singh, 2000).During the development of blood cells, the level of *PU.1* affects their differentiation. The low level of *PU.1* leads to granulocytes and high level of *PU.1* to monocytes (Singh et al., 2007).

In B-cells the level of *PU.1* has the highest level of expression in the germinal center and declines along with cell maturation (Singh et al., 2007).It is a direct (validated by several methods (RNA-seq, qRT-PCR, luciferase esej, WB) and with high score) target of miR-155 with a sequence complementary to the miR-155 seed sequence. It has been proven, that the overexpression of miR-155 leads to decrease of *PU.1* mRNA, but also the amount of SPI1 protein (Vargova et al., 2011). (Stopka et al., 2007)found, that between *PU.1* and miR-155

exists a mutual regulatory loop, increased level of miR-155 leads to inhibiting of *PU.1* function, and suppressing of *PU.1* regulated pathways then binds to miR-155 promoter and increases miR-155 expression. Our results confirm, that in leukemic cell lines, *PU.1* was highly suppressed in comparison with B-cells of healthy patients. In both cases of monoallelic and biallelic deletion, the level of expression of *PU.1* significantly rises, but in the case of single knockout the change was between one or two times fold, so not as extreme as in the case of double knockout, where the change was about five times fold (Alivernini et al., 2016).

It was previously proved, that *MYB* (v-myb myeloblastosis viral oncogene homolog) regulates expression of miR-155, concretely physically associates with the promoter of *MIR155HG* that results in stimulation of miR-155 transcription/expression in CLL cells (Vargova et al., 2011). According to this, in both cell lines the level of *MYB* expression was significantly higher compared to healthy B-cells. Which was expected, because both high levels of these genes are markers of cancerous diseases. As a result of our measurements, after monoallelic and biallelic deletion of miR-155, the expression of *MYB* lowered. Leading to assumption, that *MYB* and miR-155 are part of a feedback loop, similarly as in the case of TGF β and miR-155 (Butz et al., 2012). The level of *MYB* also significantly increases with poor prognosis of CLL.

FOXP3 is a transcription factor, which is part of regulation of miR-155 in breast cancer (Yi et al., 2018, s. 3) and works as a tumor suppressor in breast and prostate epithelia (Ladoire et al., 2011). In both our cell lines we observed that *FOXP3* is highly suppressed by miR-155 compared to expression in healthy B-cells. In our miR-155 deficient leukemic cell lines, the expression of *FOXP3* didn't changed significantly. In MEC-1 cell line (biallelic deletion) the levels rose, but the standard deviation was too high to confirm the significancy. In HG-3 cell line (monoallelic deletion) the level was almost the same as in wild type leukemic cells. Our results align with other studies and the relationship between *FOXP3* and miR-155 expressions.

CDKN1A is a gene which encodes the well-known potent cyclin-dependent kinase inhibitor p21. This gene is actively transcribed during the G1 phase of the cell cycle, binds and inhibits the activity of complexes of cyclin-cyclin dependent kinase 2 and cyclin-cyclin dependent kinase 4. This inhibitor also plays role in the S phase and DNA damage repair in the cell cycle. In our measurements, the expression of *CDKN1A* significantly changed. The most noticeable difference was observed between the levels of healthy cells and HG-3 cell line with monoallelic deletion. This is quite an interesting finding. Compared to the results of the MEC-1 cell line, the difference between wild type and biallelic deletion is significant, but not as high as in monoallelic deletion. As we know, miR-155 is involved in many pathways, therefore we

suggest, that even though the deletion in HG-3 cell line was monoallelic, it is cell line derived from CLL cells of patient with worse prognosis. Therefore higher influence on the level of *CDKN1A* expression could be initiated by another pathway that we are not aware of. According to (Gironella et al., 2007) miR-155 is a target of *TP53*. Roosbroeck *et al.* confirmed that miR-155 is involved in a feedback loop with *TP53*, with an experiment transfecting *TP53* wild-type and miR-155, which resulted in reduced expression of *TP53* gene along with reduced *CDKN1A* (p21). Based on abovementioned, our results correspond with others research findings.

CDKN2C is, similarly as *CDKN1A*, an inhibitor of cyclin-dependent kinase, specifically cyclin-dependent kinase 4 and cyclin-dependent kinase 6. Both are part of the G1 phase of the cell cycle. Similar level of expression was therefore expected also for *CDKN1A*. Our measurements show differences. The expression level of *CDKN2C* was significantly lower in comparison with healthy B-cells, independently on wild-type, monoallelic or biallelic deletion. In multiple myeloma, (Benetatos & Vartholomatos, 2012) found that miR-155 is part of processes which lead to *CDKN2A* and *CDKN2C* inactivation. We can confirm that, but the result which showed that the level of *CDKN2C* didn't rise back, was quite surprising..

Gene *GNB4* encodes a beta subunit of G proteins, which integrates signals between receptors and effector proteins. They are composed of an alpha, a beta, and a gamma subunit. In the graphs (Fig.15,16) there is a visible difference in the expression of *GNB4* in both cell lines. Compared to healthy B-cells, the level of *GNB4* was close to zero in both cell lines as the relative level of expression is low. In comparison of wild type and cells with deletion, in monoallelic type, the expression was still not measurable, but in biallelic deletion the level of *GNB4* rose significantly (this confirms that *GNB4* is miR-155 target). Therefore, double knockout is needed for a change to occur. Due to lack of any related published data explaining the effect of miR-155 on *GNB4* are available we couldn't compare/discuss our results with published.

FOS is a gene encoding transcription factor c-Fos and is a protooncogene. The Fos gene family consists of 4 members: *FOS*, *FOSB*, *FOSL1*, and *FOSL2*. These genes can dimerize with proteins of the JUN family, and as a result form the transcription factor complex AP-1. The *FOS* proteins are regulators of cell proliferation, differentiation, and transformation (Hop et al., 2018). In some cases, expression of the *FOS* gene has also been associated with apoptotic cell death (Marti et al., 1994). The expression level of the *FOS* gene is significantly lower in both cell lines compared to expression in healthy B-cells. This confirms that miR-155 is suppressing *FOS* gene. After the deletion, in both monoallelic and biallelic clones rose expression of *FOS*,

which shows that single knockout of miR-155 is sufficient for restoring the expression of *FOS* gene and its apoptotic activity. According to statistics, only in the MEC-1 cell line the change is significant, but that is because of high standard deviation in the HG-3 cell line. Currently, the role of c-fos in relation to miR-155 expression in oral lichen planus, which is a chronic mucosal inflammatory disease has been studied (Tao et al., 2019).

PRKARIA encodes regulatory subunits of the cAMP-dependent protein kinases. We found that the relative expression of *PRKARIA* gene was significantly lower in both HG-3 and MEC-1 cell line in comparison to expression in healthy B-cells (Fig.15,16). After deletion of miR-155, the expression in HG-3 rose significantly (Fig.17). On the other hand, in the MEC-1 cell line, the level of *PRKARIA* does not differ in wt vs miR-155 deficient clone (Fig.17). *PRKARIA* was proved to be a functional tumor suppressor in lung adenocarcinoma by (Wang et al., 2016, s. 1)?. Authors measured the mRNA level of *PRKARIA* and compared its expression levels in normal tissue and lung adenocarcinoma, both in a cohort of 102 patients. Significantly lower expression (mRNA and also protein) authors found in adenocarcinoma samples. These findings are in line with our results.

SHIP1 is phosphatase, which leads to inhibition of the PI3K pathway. It is a direct target of miR-155 (O'Connell et al., 2009) . It was confirmed in DLBCL (Diffuse large B-cell lymphoma in adults) cell lines, transgenic mice and also *in vitro* and *in vivo* experiments. (Lind et al., 2015) *SHIP1* is involved in B-cell maturation, and is correlated with DLBCL prognosis (Pedersen et al., 2009). In our measurement, expression of *SHIP1* was lowered in MEC-1 cell line significantly. If we focus on comparison of wild type versus monoallelic/biallelic deletion, in monoallelic, the level remains unchanged. But after biallelic deletion, the level of *SHIP1* significantly rose 3-fold change (Fig.17). We can see, that in both cell lines, *SHIP1* is highly affected by miR-155, but in order to restore normal expression, biallelic deletion is needed, but it is still not enough to gain the "normal" level. According to (Mraz & Kipps, 2013) cells with low expression of *SHIP1* have higher capacity for BCR signalling.

Further expressed gene is *hsa-miR-155*, as mentioned above, clearly deletion of 6 nucleotides within the mature sequence of miR-155, is not sufficient for complete loss of its function. In MEC-1 cell line this deletion was successful, we gained biallelic deletion (homozygous clone).

„Not- validated targets“ a *bona fide* (potential) targets of miR-155 in CLL cells

CDK14 is a gene which encodes Cyclin dependent kinase 14. It has significant involvement in tumorigenesis of cancers including hepatocellular carcinoma, gastric carcinoma and breast cancer.

CDK14 acts as a cell-cycle regulator of the Wnt signaling pathway during the G2/M phase by mediating the phosphorylation of LRP6 at 'Ser-1490', leading to the activation of the Wnt signaling pathway (Chen et al., 2019, s. 14; Ji et al., 2017). We observed, that compared to healthy B-cells, the level of *CDK14* significantly rose in wild type HG-3 cells, showing that proliferation of leukemic cells occurs more often. On the other hand, the change in MEC-1 cell line didn't occur in normal vs leukemic cells. But if we focus on the changes after deleting one or two alleles of miR-155, in the case of monoallelic deletion, no significant change happened, but biallelic deletion lowered the level of expression. We understand these results as that the change of proliferation and cell cycle occurs mostly in early stages of chronic lymphocytic leukemia and, as we mentioned before and which was also proven by Kim *et al.*, in order to observe changes in expression, deletion in both alleles has to occur.

LMNA encodes protein which is part of the nuclear lamina and therefore part of the cytoskeleton. Mutations in this gene lead to several diseases, such as familial partial lipodystrophy, Emery-Dreifuss muscular dystrophy and dilated cardiomyopathy. Our findings about the level of expression of this gene are quite interesting. Comparing the levels of normal and leukemic cells, in the HG-3 cell line, no change occurred. In the MEC-1 cell line, the level of *LMNA* slightly increased, but not significantly (Fig.16). But if we focus on the changes after deletion, in monoallelic deletion the level rose 3-fold change (Fig.17), but in the biallelic deletion the level declined (Fig.17). Both were significant. This finding shows, that the level of miR-155 can also be part of cytoskeletal forming pathways. We suggest that in this case *LMNA* may be target of miR-155 but not direct and the changes in *LMNA* are also orchestrated by other genes, which are in this case not known. In current research, there has been found link between *LMNA* and microRNAs in cardiomyopathy, but this topic hasn't been studied thoroughly yet (Calderon-Dominguez et al., 2020).

ISG15 is a gene encoding an ubiquitin-like protein, which is connected to its intracellular target proteins upon activation by interferon alpha and interferon-beta. Our measurements show, that *ISG15* is significantly changed (2-fold change) in both MEC-1 and HG-3 cell lines (Fig.17). Compared to normal expression (expression in healthy B-cells), *ISG15* was highly

suppressed in the wild type and after deletion, both levels rose again, which shows that *ISG15* is highly sensitive to the level of miR-155, when even monoallelic deletion can cause two fold change higher expression (Fig.17). Because *ISG15* is the predicted target of miR-155, no further studies were found studying the connection between *ISG15* and miR-155. To further confirm our hypothesis of *ISG15* being a target of miR-155, we suggest confirming that further by Western blot and comparing the amount of protein produced. Also, perform functional assay with delivery of siRNA and mimic *ISG15*.

LDHA is one of glucose transporters, which in breast cancer was affected by loss of miR-155, due to down-regulation of cMYC. By the UTR analysis Kim et al., 2018 found, that miR-155 directly repress *PIK3R1* and *FOXO3* genes. Their findings also show, that miR-155 is a key regulator of glucose metabolism in breast cancer. Stable expression of miR-155 showed activated glucose metabolims, on the other hand, inhibition of miR-155 resulted in reducing *in vivo* tumor growth with retarded glucose metabolism. (Kim et al., 2018) found, that cells with single miR-155 knockout increase glucose uptake and lactate production compared to cells with double miR-155 knockout. Therefore, double knockout is crucial for successful affecting of metabolic pathways. And also showed, that PIK3R1-PDK1/AKT-FOXO3 pathway is affected directly by miR-155. These findings were confirmed also *in vivo*. In their research, results of miR-155 expression by monoallelic/single knockout and biallelic/double knockout were similar compared to ours.

Therefore we were expecting the same change in expression of *LDHA* gene, one of our predicted targets. Unfortunately this significant change was observed only in MEC-1 cell line – biallelic deletion and cells with poorer prognosis (Fig.16). For this reason we have to decline our hypothesis, that *LDHA* may be a direct target of miR-155.

RPS29 is a gene, which encodes ribosomal protein S29. This protein is part of 40S subunit and is located in the cytoplasm. Variable expression of this gene was observed in colorectal cancers, but no connection between the level of expression and the severity of the disease has been confirmed (Takemasa et al., 2012). *RPS29* is one of our potential targets of miR-155, compared to the normal healthy B-cell expression there are significant changes (Fig.15). In the HG-3 cell line the expression of *RPS29* was highly and significantly suppressed, the same effect we can observe in the MEC-1 cell line. Comparing the before and after deletion, in monoallelic (HG-3) the level slightly rose, but in biallelic (MEC-1) the level lowered (Fig.17). Based on our results, the *RPS29* is most likely target gene of miR-155, but further studies are needed, for example the *in silico* analysis of the seed region in *RPS29* gene, or *in*

in vitro analysis by Western blot. Further, the functional assays with siRNA/mimics for RPS29 mRNA would confirm or refute our hypothesis that RPS29 is a target of miR-155. Unfortunately, there were no studies specifically focused on finding a connection between this gene and miR-155.

TMSB4X - Thymosin beta 4 X-linked encodes an actin sequestering protein which has a role in the regulation of actin polymerization. This protein is involved in cell proliferation, migration and differentiation. In our results, the level of *TMSB4X* was significantly lower in comparison with healthy B-cells. On the other hand, the level rose after deletion just in the monoallelic clone, which is doubtful. Based on Seitz, this effect can happen just based on the complexity of miR-155 and its targets. Therefore confirming *TMSB4X* as a target is doubtful. Further studies, ideally *in vivo*, would have to be done.

In conclusion, we have identified potential targets of miR-155, which are *ISG15* and *RPS29*. To be able to see some permanent changes in the gene expression of miR-155, there's need for biallelic deletion (Kim et al., 2018).

To confirm that, further experiments should be performed. Possibilities are *in silico* finding of seed region in these genes for miR-155. Another option is performing Western blot and comparing the levels of these proteins at proteasome level or *in vivo* inducing higher levels of miR-155, comparing it to normal tissue levels and also seeing the result after using anti-miR treatment. Furthermore, as mentioned above, performing functional assays based on the delivery of siRNA/mimics of ISG15 and RPS29 will provide us evidence about their target role in relation to miR-155. Also, luciferase assay should be considered.

Currently, treatment of Diffuse large B-cell lymphoma was done in 2020, which showed that Cobomarsen, an oligonucleotide inhibitor of miR-155, slows tumor growth *in vitro* and also *in vivo*. The results showed that the tumor growth was stabilized and no toxic effects were observed on patients (Anastasiadou et al., 2021).

It was also found, that Anti-MiR-155 treatment along with chemotherapy helps with enduring the resistance to chemotherapy *in vivo* in lung cancers (Van Roosbroeck et al., 2017). Therefore, using anti-miR-155 treatment is surely beneficial, but not just as a single agent, but together with chemotherapy treatment, because the anti-miR-155-targeted therapies help to overcome drug resistance (Van Roosbroeck et al., 2017).

Nevertheless, experiments with manipulating the *in vitro* levels of miR-155 (in this case by CRISPR/Cas9 tool) in the leukemic cells represents valuable model for study of anti-miRNA therapy. Our results are very preliminary but should provide some insight into molecular changes at the mRNA/miRNA level.

6. Conclusion

We successfully gained a monoallelic clone by CRISPR/Cas9 gene editing of *hsa-miR-155* in the HG-3 cell line. We executed further experiments, such as measurement of the cell proliferation and viability of HG-3 and MEC-1 cell lines, which showed, that deleting of miR-155 lowers the level of proliferation, even in monoallelic deletion. In terms of viability, we didn't observe any significant changes.

We gained different levels of expressed target genes and predicted target genes of *hsa-miR-155* by qRT-PCR in both of these cell lines, and monoallelic and biallelic knockout clones, and compared them with healthy B-cell levels of expression. Between validated genes with lower expression in leukemic cells, compared to healthy B-cells, we observed *PU.1*, cyclin dependent kinase inhibitor - *CDKN2C*, *GNB4* – gene encoding beta subunit of G protein, transcription factor *FOS*, *PRKARIA*, *SHIP1* and *FOXP3*. After deletion, we didn't observe significant changes in *FOXP3*, but it may be caused by higher standard deviation.

Genes which showed higher expression in leukemic cells compared to healthy B-cells were – *MYB* and cyclin-dependent kinase inhibitor *CDKN1A*.

We were successful in identifying probable targets of miR-155. Those which showed significant changes in their expression were – *ISG15* and *RPS29*. For further confirmation of these targets, we suggest *in silico* confirmation by finding a seed sequence for miR-155 or *in vivo* experiments, which would confirm our findings by change of expression level.

7. References

- Alivernini, S., Kurowska-Stolarska, M., Tolusso, B., Benvenuto, R., Elmesmari, A., Canestri, S., Petricca, L., Mangoni, A., Fedele, A. L., Di Mario, C., Gigante, M. R., Gremese, E., McInnes, I. B., & Ferraccioli, G. (2016). MicroRNA-155 influences B-cell function through PU.1 in rheumatoid arthritis. *Nature Communications*, 7(1), 12970. <https://doi.org/10.1038/ncomms12970>
- Almeida, M. I., Reis, R. M., & Calin, G. A. (2011). MicroRNA history: Discovery, recent applications, and next frontiers. *Mutation Research/Fundamental and Molecular Mechanisms of Mutagenesis*, 717(1), 1–8. <https://doi.org/10.1016/j.mrfmmm.2011.03.009>
- Anastasiadou, E., Seto, A. G., Beatty, X., Hermreck, M., Gilles, M.-E., Stroopinsky, D., Pinter-Brown, L. C., Pestano, L., Marchese, C., Avigan, D., Trivedi, P., Escolar, D. M., Jackson, A. L., & Slack, F. J. (2021). Cobomarsen, an Oligonucleotide Inhibitor of miR-155, Slows DLBCL Tumor Cell Growth In Vitro and In Vivo. *Clinical cancer research : an official journal of the American Association for Cancer Research*, 27(4), 1139–1149. <https://doi.org/10.1158/1078-0432.CCR-20-3139>
- Benetatos, L., & Vartholomatos, G. (2012). Deregulated microRNAs in multiple myeloma: MicroRNAs in Multiple Myeloma. *Cancer*, 118(4), 878–887. <https://doi.org/10.1002/cncr.26297>
- Butz, H., Rácz, K., Hunyady, L., & Patócs, A. (2012). Crosstalk between TGF- β signaling and the microRNA machinery. *Trends in Pharmacological Sciences*, 33(7), 382–393. <https://doi.org/10.1016/j.tips.2012.04.003>
- Calderon-Dominguez, M., Belmonte, T., Quezada-Feijoo, M., Ramos-Sánchez, M., Fernández-Armenta, J., Pérez-Navarro, A., Cesar, S., Peña-Peña, L., Vea, À., Llorente-Cortés, V., Mangas, A., de Gonzalo-Calvo, D., & Toro, R. (2020). Emerging role of microRNAs in dilated cardiomyopathy: Evidence regarding etiology. *Translational Research*, 215, 86–101. <https://doi.org/10.1016/j.trsl.2019.08.007>
- Carthew, R. W., & Sontheimer, E. J. (2009). Origins and Mechanisms of miRNAs and siRNAs. *Cell*, 136(4), 642–655. <https://doi.org/10.1016/j.cell.2009.01.035>
- DeKoter, R. P., & Singh, H. (2000). Regulation of B lymphocyte and macrophage development by graded expression of PU.1. *Science (New York, N.Y.)*, 288(5470), 1439–1441. <https://doi.org/10.1126/science.288.5470.1439>
- Dorsett, Y., McBride, K. M., Jankovic, M., Gazumyan, A., Thai, T.-H., Robbiani, D. F., Di Virgilio, M., San-Martin, B. R., Heidkamp, G., Schwickert, T. A., Eisenreich, T., Rajewsky, K., & Nussenzweig, M. C. (2008). MicroRNA-155 Suppresses Activation-Induced Cytidine Deaminase-Mediated Myc-Igh Translocation. *Immunity*, 28(5), 630–638. <https://doi.org/10.1016/j.immuni.2008.04.002>
- Eis, P. S., Tam, W., Sun, L., Chadburn, A., Li, Z., Gomez, M. F., Lund, E., & Dahlberg, J. E. (2005). Accumulation of miR-155 and BIC RNA in human B cell lymphomas. *Proceedings of the National Academy of Sciences of the United States of America*, 102(10), 3627–3632. <https://doi.org/10.1073/pnas.0500613102>
- Fabbri, M., & Croce, C. M. (2011). Role of microRNAs in lymphoid biology and disease. *Current Opinion in Hematology*, 18(4), 266–272. PubMed. <https://doi.org/10.1097/MOH.0b013e3283476012>
- Fahl, S. P., Crittenden, R. B., Allman, D., & Bender, T. P. (2009). C-Myb is required for pro-B cell differentiation. *Journal of Immunology (Baltimore, Md.: 1950)*, 183(9), 5582–5592. <https://doi.org/10.4049/jimmunol.0901187>

- Fernando, T. R., Rodriguez-Malave, N. I., & Rao, D. S. (2012). MicroRNAs in B cell development and malignancy. *Journal of Hematology & Oncology*, 5(1), 7. <https://doi.org/10.1186/1756-8722-5-7>
- García-Tuñón, I., Hernández-Sánchez, M., Ordoñez, J. L., Alonso-Pérez, V., Álamo-Quijada, M., Benito, R., Guerrero, C., Hernández-Rivas, J. M., & Sánchez-Martín, M. (2017). The CRISPR/Cas9 system efficiently reverts the tumorigenic ability of BCR/ABL in vitro and in a xenograft model of chronic myeloid leukemia. *Oncotarget*, 8(16), 26027–26040. <https://doi.org/10.18632/oncotarget.15215>
- Gatto, G., Rossi, A., Rossi, D., Kroening, S., Bonatti, S., & Mallardo, M. (2008). Epstein-Barr virus latent membrane protein 1 trans-activates miR-155 transcription through the NF-kappaB pathway. *Nucleic Acids Research*, 36(20), 6608–6619. <https://doi.org/10.1093/nar/gkn666>
- Gavin, M. A., Rasmussen, J. P., Fontenot, J. D., Vasta, V., Manganiello, V. C., Beavo, J. A., & Rudensky, A. Y. (2007). Foxp3-dependent programme of regulatory T-cell differentiation. *Nature*, 445(7129), 771–775. <https://doi.org/10.1038/nature05543>
- Georgantas, R. W., Hildreth, R., Morisot, S., Alder, J., Liu, C., Heimfeld, S., Calin, G. A., Croce, C. M., & Civin, C. I. (2007). CD34+ hematopoietic stem-progenitor cell microRNA expression and function: A circuit diagram of differentiation control. *Proceedings of the National Academy of Sciences of the United States of America*, 104(8), 2750–2755. <https://doi.org/10.1073/pnas.0610983104>
- Gironella, M., Seux, M., Xie, M.-J., Cano, C., Tomasini, R., Gommeaux, J., Garcia, S., Nowak, J., Yeung, M. L., Jeang, K.-T., Chaix, A., Fazli, L., Motoo, Y., Wang, Q., Rocchi, P., Russo, A., Gleave, M., Dagorn, J.-C., Iovanna, J. L., ... Dusetti, N. J. (2007). Tumor protein 53-induced nuclear protein 1 expression is repressed by miR-155, and its restoration inhibits pancreatic tumor development. *Proceedings of the National Academy of Sciences of the United States of America*, 104(41), 16170–16175. <https://doi.org/10.1073/pnas.0703942104>
- Greig, K. T., de Graaf, C. A., Murphy, J. M., Carpinelli, M. R., Pang, S. H. M., Frampton, J., Kile, B. T., Hilton, D. J., & Nutt, S. L. (2010). Critical roles for c-Myb in lymphoid priming and early B-cell development. *Blood*, 115(14), 2796–2805. <https://doi.org/10.1182/blood-2009-08-239210>
- Grishok, A., Pasquinelli, A. E., Conte, D., Li, N., Parrish, S., Ha, I., Baillie, D. L., Fire, A., Ruvkun, G., & Mello, C. C. (2001). Genes and mechanisms related to RNA interference regulate expression of the small temporal RNAs that control *C. elegans* developmental timing. *Cell*, 106(1), 23–34. [https://doi.org/10.1016/s0092-8674\(01\)00431-7](https://doi.org/10.1016/s0092-8674(01)00431-7)
- Guo, H., Ingolia, N. T., Weissman, J. S., & Bartel, D. P. (2010). Mammalian microRNAs predominantly act to decrease target mRNA levels. *Nature*, 466(7308), 835–840. <https://doi.org/10.1038/nature09267>
- Helgason, C. D., Kalberer, C. P., Damen, J. E., Chappel, S. M., Pineault, N., Krystal, G., & Humphries, R. K. (2000). A dual role for Src homology 2 domain-containing inositol-5-phosphatase (SHIP) in immunity: Aberrant development and enhanced function of B lymphocytes in ship ^{-/-} mice. *The Journal of Experimental Medicine*, 191(5), 781–794. <https://doi.org/10.1084/jem.191.5.781>
- Hop, H. T., Arayan, L. T., Huy, T. X. N., Reyes, A. W. B., Vu, S. H., Min, W., Lee, H. J., Rhee, M. H., Chang, H. H., & Kim, S. (2018). The Key Role of c-Fos for Immune Regulation and Bacterial Dissemination in Brucella Infected Macrophage. *Frontiers in Cellular and Infection Microbiology*, 8. <https://www.frontiersin.org/article/10.3389/fcimb.2018.00287>
- Huskova, H., Korecka, K., Karban, J., Vargova, J., Vargova, K., Dusilkova, N., Trneny, M., & Stopka, T. (2015). Oncogenic microRNA-155 and its target PU.1: An integrative gene

- expression study in six of the most prevalent lymphomas. *International Journal of Hematology*, 102(4), 441–450. <https://doi.org/10.1007/s12185-015-1847-4>
- Hutvagner, G., McLachlan, J., Pasquinelli, A. E., Bálint, E., Tuschl, T., & Zamore, P. D. (2001). A cellular function for the RNA-interference enzyme Dicer in the maturation of the let-7 small temporal RNA. *Science (New York, N.Y.)*, 293(5531), 834–838. <https://doi.org/10.1126/science.1062961>
- Chen, L., Wang, Y., Jiang, W., Ni, R., Wang, Y., & Ni, S. (2019). CDK14 involvement in proliferation migration and invasion of esophageal cancer. *Annals of Translational Medicine*, 7(22), 681. <https://doi.org/10.21037/atm.2019.11.105>
- Chen, L., Widhopf, G., Huynh, L., Rassenti, L., Rai, K. R., Weiss, A., & Kipps, T. J. (2002). Expression of ZAP-70 is associated with increased B-cell receptor signaling in chronic lymphocytic leukemia. *Blood*, 100(13), 4609–4614. <https://doi.org/10.1182/blood-2002-06-1683>
- Chiorazzi, N., Rai, K. R., & Ferrarini, M. (2005). Chronic lymphocytic leukemia. *The New England Journal of Medicine*, 352(8), 804–815. <https://doi.org/10.1056/NEJMra041720>
- Chronic lymphocytic leukaemia – atypical pleomorphic variant (mixed cell type)—CELL - Atlas of Haematological Cytology*. (b.r.). Získáno 30. listopad 2020, z <http://www.leukemia-cell.org/atlas/index.php?pg=images--mature-b-cell-neoplasms--chronic-lymphocytic-leukaemia--atypical-pleomorphic-variant-mixed-cell-type#1>
- Ji, Q., Xu, X., Li, L., Goodman, S. B., Bi, W., Xu, M., Xu, Y., Fan, Z., Maloney, W. J., Ye, Q., & Wang, Y. (2017). MiR-216a inhibits osteosarcoma cell proliferation, invasion and metastasis by targeting CDK14. *Cell Death & Disease*, 8(10), e3103–e3103. <https://doi.org/10.1038/cddis.2017.499>
- Kim, S., Lee, E., Jung, J., Lee, J. W., Kim, H. J., Kim, J., Yoo, H. J., Lee, H. J., Chae, S. Y., Jeon, S. M., Son, B. H., Gong, G., Sharan, S. K., & Chang, S. (2018). MicroRNA-155 positively regulates glucose metabolism via PIK3R1-FOXO3a-cMYC axis in breast cancer. *Oncogene*, 37(22), 2982–2991. <https://doi.org/10.1038/s41388-018-0124-4>
- Kluiver, J., Poppema, S., de Jong, D., Blokzijl, T., Harms, G., Jacobs, S., Kroesen, B.-J., & van den Berg, A. (2005). BIC and miR-155 are highly expressed in Hodgkin, primary mediastinal and diffuse large B cell lymphomas. *The Journal of Pathology*, 207(2), 243–249. <https://doi.org/10.1002/path.1825>
- Ladoire, S., Arnould, L., Mignot, G., Coudert, B., Rébé, C., Chalmin, F., Vincent, J., Bruchard, M., Chauffert, B., Martin, F., Fumoleau, P., & Ghiringhelli, F. (2011). Presence of Foxp3 expression in tumor cells predicts better survival in HER2-overexpressing breast cancer patients treated with neoadjuvant chemotherapy. *Breast Cancer Research and Treatment*, 125(1), 65–72. <https://doi.org/10.1007/s10549-010-0831-1>
- Lind, E. F., Millar, D. G., Dissanayake, D., Savage, J. C., Grimshaw, N. K., Kerr, W. G., & Ohashi, P. S. (2015). MiR-155 Upregulation in Dendritic Cells Is Sufficient To Break Tolerance In Vivo by Negatively Regulating SHIP1. *The Journal of Immunology*, 195(10), 4632–4640. <https://doi.org/10.4049/jimmunol.1302941>
- Livak, K. J., & Schmittgen, T. D. (2001). Analysis of Relative Gene Expression Data Using Real-Time Quantitative PCR and the 2⁻ $\Delta\Delta$ CT Method. *Methods*, 25(4), 402–408. <https://doi.org/10.1006/meth.2001.1262>
- Lu, D., Nakagawa, R., Lazzaro, S., Staudacher, P., Abreu-Goodger, C., Henley, T., Boiani, S., Leyland, R., Galloway, A., Andrews, S., Butcher, G., Nutt, S. L., Turner, M., & Vigorito, E. (2014). The miR-155-PU.1 axis acts on Pax5 to enable efficient terminal B cell differentiation. *The Journal of Experimental Medicine*, 211(11), 2183–2198. <https://doi.org/10.1084/jem.20140338>

- Lu, F., Weidmer, A., Liu, C.-G., Volinia, S., Croce, C. M., & Lieberman, P. M. (2008). Epstein-Barr virus-induced miR-155 attenuates NF-kappaB signaling and stabilizes latent virus persistence. *Journal of Virology*, 82(21), 10436–10443. <https://doi.org/10.1128/JVI.00752-08>
- Marson, A., Kretschmer, K., Frampton, G. M., Jacobsen, E. S., Polansky, J. K., MacIsaac, K. D., Levine, S. S., Fraenkel, E., von Boehmer, H., & Young, R. A. (2007). Foxp3 occupancy and regulation of key target genes during T-cell stimulation. *Nature*, 445(7130), 931–935. <https://doi.org/10.1038/nature05478>
- Marti, A., Jehn, B., Costello, E., Keon, N., Ke, G., Martin, F., & Jaggi, R. (1994). Protein kinase A and AP-1 (c-Fos/JunD) are induced during apoptosis of mouse mammary epithelial cells. *Oncogene*, 9(4), 1213–1223.
- Mashima, R. (2015). Physiological roles of miR-155. *Immunology*, 145(3), 323–333. <https://doi.org/10.1111/imm.12468>
- Mraz, M., & Kipps, T. J. (2013). MicroRNAs and B cell receptor signaling in chronic lymphocytic leukemia. *Leukemia & Lymphoma*, 54(8), 1836–1839. <https://doi.org/10.3109/10428194.2013.796055>
- Murphy, D. J., Junttila, M. R., Pouyet, L., Karnezis, A., Shchors, K., Bui, D. A., Brown-Swigart, L., Johnson, L., & Evan, G. I. (2008). Distinct thresholds govern Myc's biological output in vivo. *Cancer Cell*, 14(6), 447–457. <https://doi.org/10.1016/j.ccr.2008.10.018>
- O'Connell, R. M., Chaudhuri, A. A., Rao, D. S., & Baltimore, D. (2009). Inositol phosphatase SHIP1 is a primary target of miR-155. *Proceedings of the National Academy of Sciences*, 106(17), 7113–7118. <https://doi.org/10.1073/pnas.0902636106>
- O'Connell, R. M., Taganov, K. D., Boldin, M. P., Cheng, G., & Baltimore, D. (2007). MicroRNA-155 is induced during the macrophage inflammatory response. *Proceedings of the National Academy of Sciences of the United States of America*, 104(5), 1604–1609. <https://doi.org/10.1073/pnas.0610731104>
- O'Connell, R. M., Zhao, J. L., & Rao, D. S. (2011). MicroRNA function in myeloid biology. *Blood*, 118(11), 2960–2969. PubMed. <https://doi.org/10.1182/blood-2011-03-291971>
- O'Donnell, K. A., Wentzel, E. A., Zeller, K. I., Dang, C. V., & Mendell, J. T. (2005). C-Myc-regulated microRNAs modulate E2F1 expression. *Nature*, 435(7043), 839–843. <https://doi.org/10.1038/nature03677>
- Pospisil, V., Vargova, K., Kokavec, J., Rybarova, J., Savvulidi, F., Jonasova, A., Necas, E., Zavadil, J., Laslo, P., & Stopka, T. (2011). Epigenetic silencing of the oncogenic miR-17-92 cluster during PU.1-directed macrophage differentiation: Pu.1/Egr2/Jarid1b pathway silences miR-17-92 cluster. *The EMBO Journal*, 30(21), 4450–4464. <https://doi.org/10.1038/emboj.2011.317>
- Rodriguez, A., Vigorito, E., Clare, S., Warren, M. V., Couttet, P., Soond, D. R., van Dongen, S., Grocock, R. J., Das, P. P., Miska, E. A., Vetrie, D., Okkenhaug, K., Enright, A. J., Dougan, G., Turner, M., & Bradley, A. (2007). Requirement of bic/microRNA-155 for Normal Immune Function. *Science*, 316(5824), 608–611. <https://doi.org/10.1126/science.1139253>
- Seiffert, M., Stilgenbauer, S., Döhner, H., & Lichter, P. (2007). Efficient nucleofection of primary human B cells and B-CLL cells induces apoptosis, which depends on the microenvironment and on the structure of transfected nucleic acids. *Leukemia*, 21(9), 1977–1983. <https://doi.org/10.1038/sj.leu.2404863>
- Seitz, H. (2017). Issues in current microRNA target identification methods. *RNA Biology*, 14(7), 831–834. <https://doi.org/10.1080/15476286.2017.1320469>

- Singh, H., Pongubala, J. M. R., & Medina, K. L. (2007). Gene regulatory networks that orchestrate the development of B lymphocyte precursors. *Advances in Experimental Medicine and Biology*, 596, 57–62. https://doi.org/10.1007/0-387-46530-8_5
- Stopka, T., Vargova, K., Kokavec, J., Pospisil, V., Curik, N., Burda, P., Skoultchi, A. I., & Zavadil, J. (2007). Mutual Regulatory Loop between miR-155 and PU.1 Is a Candidate Pathogenesis Factor in CLL. *Blood*, 110(11), 1130. <https://doi.org/10.1182/blood.V110.11.1130.1130>
- Takemasa, I., Kittaka, N., Hitora, T., Watanabe, M., Matsuo, E.-I., Mizushima, T., Ikeda, M., Yamamoto, H., Sekimoto, M., Nishimura, O., Doki, Y., & Mori, M. (2012). Potential biological insights revealed by an integrated assessment of proteomic and transcriptomic data in human colorectal cancer. *International Journal of Oncology*, 40(2), 551–559. <https://doi.org/10.3892/ijo.2011.1244>
- Tao, Y., Ai, R., Hao, Y., Jiang, L., Dan, H., Ji, N., Zeng, X., Zhou, Y., & Chen, Q. (2019). Role of miR-155 in immune regulation and its relevance in oral lichen planus (Review). *Experimental and Therapeutic Medicine*, 17(1), 575–586. <https://doi.org/10.3892/etm.2018.7019>
- Teng, G., Hakimpour, P., Landgraf, P., Rice, A., Tuschl, T., Casellas, R., & Papavasiliou, F. N. (2008). MicroRNA-155 is a negative regulator of activation-induced cytidine deaminase. *Immunity*, 28(5), 621–629. <https://doi.org/10.1016/j.immuni.2008.03.015>
- Thai, T.-H., Calado, D. P., Casola, S., Ansel, K. M., Xiao, C., Xue, Y., Murphy, A., Frendewey, D., Valenzuela, D., Kutok, J. L., Schmidt-Suppran, M., Rajewsky, N., Yancopoulos, G., Rao, A., & Rajewsky, K. (2007). Regulation of the germinal center response by microRNA-155. *Science (New York, N.Y.)*, 316(5824), 604–608. <https://doi.org/10.1126/science.1141229>
- Thomas, M. D., Kremer, C. S., Ravichandran, K. S., Rajewsky, K., & Bender, T. P. (2005). C-Myb is critical for B cell development and maintenance of follicular B cells. *Immunity*, 23(3), 275–286. <https://doi.org/10.1016/j.immuni.2005.08.005>
- Tili, E., Croce, C. M., & Michaille, J.-J. (2009). miR-155: On the crosstalk between inflammation and cancer. *International Reviews of Immunology*, 28(5), 264–284. <https://doi.org/10.1080/08830180903093796>
- Tili, E., Michaille, J.-J., Cimino, A., Costinean, S., Dumitru, C. D., Adair, B., Fabbri, M., Alder, H., Liu, C. G., Calin, G. A., & Croce, C. M. (2007). Modulation of miR-155 and miR-125b levels following lipopolysaccharide/TNF-alpha stimulation and their possible roles in regulating the response to endotoxin shock. *Journal of Immunology (Baltimore, Md.: 1950)*, 179(8), 5082–5089. <https://doi.org/10.4049/jimmunol.179.8.5082>
- Van Roosbroeck, K., Fanini, F., Setoyama, T., Ivan, C., Rodriguez-Aguayo, C., Fuentes-Mattei, E., Xiao, L., Vannini, I., Redis, R. S., D'Abundo, L., Zhang, X., Nicoloso, M. S., Rossi, S., Gonzalez-Villasana, V., Rupaimoole, R., Ferracin, M., Morabito, F., Neri, A., Ruvolo, P. P., ... Calin, G. A. (2017). Combining Anti-Mir-155 with Chemotherapy for the Treatment of Lung Cancers. *Clinical Cancer Research: An Official Journal of the American Association for Cancer Research*, 23(11), 2891–2904. <https://doi.org/10.1158/1078-0432.CCR-16-1025>
- Vargova, K., Curik, N., Burda, P., Basova, P., Kulvait, V., Pospisil, V., Savvulidi, F., Kokavec, J., Necas, E., Berkova, A., Obrtlíkova, P., Karban, J., Mraz, M., Pospisilova, S., Mayer, J., Trneny, M., Zavadil, J., & Stopka, T. (2011). MYB transcriptionally regulates the miR-155 host gene in chronic lymphocytic leukemia. *Blood*, 117(14), 3816–3825. <https://doi.org/10.1182/blood-2010-05-285064>
- Vargova, K., Pesta, M., Obrtlíkova, P., Dusilkova, N., Minarik, L., Vargova, J., Berkova, A., Zemanova, Z., Michalova, K., Spacek, M., Trneny, M., & Stopka, T. (2017). MiR-155/miR-150 network regulates progression through the disease phases of chronic

- lymphocytic leukemia. *Blood Cancer Journal*, 7(7), e585–e585. <https://doi.org/10.1038/bcj.2017.63>
- Vigorito, E., Kohlhaas, S., Lu, D., & Leyland, R. (2013). miR-155: An ancient regulator of the immune system. *Immunological Reviews*, 253(1), 146–157. <https://doi.org/10.1111/imr.12057>
- Vigorito, E., Perks, K. L., Abreu-Goodger, C., Bunting, S., Xiang, Z., Kohlhaas, S., Das, P. P., Miska, E. A., Rodriguez, A., Bradley, A., Smith, K. G. C., Rada, C., Enright, A. J., Toellner, K.-M., MacLennan, I. C. M., & Turner, M. (2007). MicroRNA-155 Regulates the Generation of Immunoglobulin Class-Switched Plasma Cells. *Immunity*, 27(6), 847–859. <https://doi.org/10.1016/j.immuni.2007.10.009>
- Wang, S., Cheng, Y., Zheng, Y., He, Z., Chen, W., Zhou, W., Duan, C., & Zhang, C. (2016). PRKAR1A is a functional tumor suppressor inhibiting ERK/Snai1/E-cadherin pathway in lung adenocarcinoma. *Scientific Reports*, 6, 39630. <https://doi.org/10.1038/srep39630>
- Winter, J., Jung, S., Keller, S., Gregory, R. I., & Diederichs, S. (2009). Many roads to maturity: MicroRNA biogenesis pathways and their regulation. *Nature Cell Biology*, 11(3), 228–234. <https://doi.org/10.1038/ncb0309-228>
- Xiao, M., Li, J., Li, W., Wang, Y., Wu, F., Xi, Y., Zhang, L., Ding, C., Luo, H., Li, Y., Peng, L., Zhao, L., Peng, S., Xiao, Y., Dong, S., Cao, J., & Yu, W. (2016). MicroRNAs activate gene transcription epigenetically as an enhancer trigger. *RNA Biology*, 14(10), 1326–1334. <https://doi.org/10.1080/15476286.2015.1112487>
- Xu, L., Leng, H., Shi, X., Ji, J., Fu, J., & Leng, H. (2017). MiR-155 promotes cell proliferation and inhibits apoptosis by PTEN signaling pathway in the psoriasis. *Biomedicine & Pharmacotherapy*, 90, 524–530. <https://doi.org/10.1016/j.biopha.2017.03.105>
- Yi, B., Li, M., Liu, Y., & Liu, R. (2018). Abstract 4429: FOXP3 transcriptional regulation of MicroRNAs in human breast cancer. *Cancer Research*, 78(13_Supplement), 4429. <https://doi.org/10.1158/1538-7445.AM2018-4429>
- Yin, Q., McBride, J., Fewell, C., Lacey, M., Wang, X., Lin, Z., Cameron, J., & Flemington, E. K. (2008). MicroRNA-155 Is an Epstein-Barr Virus-Induced Gene That Modulates Epstein-Barr Virus-Regulated Gene Expression Pathways. *Journal of Virology*, 82(11), 5295–5306. <https://doi.org/10.1128/JVI.02380-07>
- Yin, Q., Wang, X., McBride, J., Fewell, C., & Flemington, E. (2008). B-cell receptor activation induces BIC/miR-155 expression through a conserved AP-1 element. *The Journal of Biological Chemistry*, 283(5), 2654–2662. <https://doi.org/10.1074/jbc.M708218200>
- Yu, H., Xu, W., Gong, F., Chi, B., Chen, J., & Zhou, L. (2017). MicroRNA-155 regulates the proliferation, cell cycle, apoptosis and migration of colon cancer cells and targets CBL. *Experimental and Therapeutic Medicine*, 14(5), 4053–4060. <https://doi.org/10.3892/etm.2017.5085>
- Zhang, S., Shen, J., Li, D., & Cheng, Y. (2021). Strategies in the delivery of Cas9 ribonucleoprotein for CRISPR/Cas9 genome editing. *Theranostics*, 11(2), 614–648. <https://doi.org/10.7150/thno.47007>
- Zheng, Y., & Rudensky, A. Y. (2007). Foxp3 in control of the regulatory T cell lineage. *Nature Immunology*, 8(5), 457–462. <https://doi.org/10.1038/ni1455>

Internet resources

<https://www.genecards.org/>

<http://www.mirbase.org/>

<https://rnacentral.org/>